Stem Cell Reports
Article

OPEN ACCESS

The Bile Acid Nuclear Receptor FXRα Is a Critical Regulator of Mouse Germ Cell Fate

Emmanuelle Martinot,[1] Lauriane Sèdes,[1] Marine Baptissart,[1] Hélène Holota,[1] Betty Rouaisnel,[1] Christelle Damon-Soubeyrand,[1,2] Angélique De Haze,[1,2] Jean-Paul Saru,[1,2] Christelle Thibault-Carpentier,[3] Céline Keime,[3] Jean-Marc A. Lobaccaro,[1,2] Silvère Baron,[1,2] Gérard Benoit,[4] Françoise Caira,[1] Claude Beaudoin,[1] and David H. Volle[1,*]

[1]INSERM U 1103, Université Clermont Auvergne, CNRS UMR 6293, Laboratoire GReD, 28 Place Henri Dunant, 63000 Clermont-Ferrand, France
[2]Centre de Recherche en Nutrition Humaine d'Auvergne, 63000 Clermont-Ferrand, France
[3]IGBMC - CNRS UMR 7104 - Inserm U 964, 1 BP 10142, 67404 Illkirch Cedex, France
[4]Laboratoire de Biologie Moléculaire de la Cellule, Ecole normale supérieure de Lyon, UMR5239 CNRS/ENS Lyon/UCBL/HCL, 46, allée d'Italie, 69364 Lyon Cedex 07, France
*Correspondence: david.volle@inserm.fr
http://dx.doi.org/10.1016/j.stemcr.2017.05.036

SUMMARY

Spermatogenesis is the process by which spermatozoa are generated from spermatogonia. This cell population is heterogeneous, with self-renewing spermatogonial stem cells (SSCs) and progenitor spermatogonia that will continue on a path of differentiation. Only SSCs have the ability to regenerate and sustain spermatogenesis. This makes the testis a good model to investigate stem cell biology. The Farnesoid X Receptor alpha (FXRα) was recently shown to be expressed in the testis. However, its global impact on germ cell homeostasis has not yet been studied. Here, using a phenotyping approach in *Fxrα*$^{-/-}$ mice, we describe unexpected roles of FXRα on germ cell physiology independent of its effects on somatic cells. FXRα helps establish and maintain an undifferentiated germ cell pool and in turn influences male fertility. FXRα regulates the expression of several pluripotency factors. Among these, in vitro approaches show that FXRα controls the expression of the pluripotency marker Lin28 in the germ cells.

INTRODUCTION

Major functions of the testis include production of gametes and male hormones. Testosterone synthesized by the Leydig cells influences male fertility through its involvement in testis development, attainment of puberty, and maintenance of spermatogenesis (Wilson et al., 2002). Gamete production occurs in the seminiferous tubules and depends on the physiology of the Sertoli cells, which ensure structural and nutritional support for the germ cell lineage. Throughout the adult life of mammals such as the mouse (used in this study), spermatogenesis relies on the existence of a pool of spermatogonial stem cells (SSCs). It involves a delicate balance between self-renewal mitosis and differentiation (Lui et al., 2003). However, the population of undifferentiated spermatogonia is heterogeneous. Subpopulations of stem cells and progenitors have been defined (Griswold and Oatley, 2013; Oatley and Brinster, 2012). Stem cells have the ability to regenerate and sustain spermatogenesis, whereas progenitors lack regenerative capacity. An undifferentiated type A spermatogonia population comprises both SSCs and progenitors (de Rooij and Russell, 2000). In mice, they can be classified into single cells (As), pairs of cells (Apair), or aligned cells (Aal4–16). It is considered that the SSC pool is composed of As cells, so that Apair cells are progenitors (Huckins and Oakberg, 1978). However, it has been suggested that spermatogonia with stem cell properties are more diverse than As spermatogonia (Nakagawa et al., 2010; Hara et al., 2014). A clear identification of these two cell populations (SSCs and progenitors) is still needed. The mechanisms involved in the regulation of the homeostasis of these specific cellular pools also remain to be defined.

Recently, the nuclear receptor Farnesoid X Receptor α (FXRα; NR1H4) was shown to be a regulator of the endocrine function of the testis. The activation of the FXRα pathways in Leydig cells, by administration of the specific synthetic agonist GW4064, causes a decrease in testosterone synthesis, which in turn induces an androgen-dependent apoptosis of germ cells. This is associated with impaired sexual maturation of males and ensuing infertility (Baptissart et al., 2016).

Fxrα has also been detected in the seminiferous tubules (Volle et al., 2007a). However, the potential impacts of FXRα signaling pathways on testicular physiology, particularly in exocrine function, remain unclear. The present study shows that FXRα defines long-term reproductive capacity of males. Here, using a phenotyping approach in *Fxrα*$^{-/-}$ mice, we identified unexpected roles of this receptor in the testis. Almost all cell types in the testis are affected by a lack of FXRα. The present data suggest that FXRα acts on germ cells independently of its effects on Leydig and/or Sertoli cells. This is supported by evidence that FXRα signaling pathways help define transcriptome features of undifferentiated type A spermatogonia. In *Fxrα*$^{-/-}$ males, the maintenance of fertility capacities resulting from high

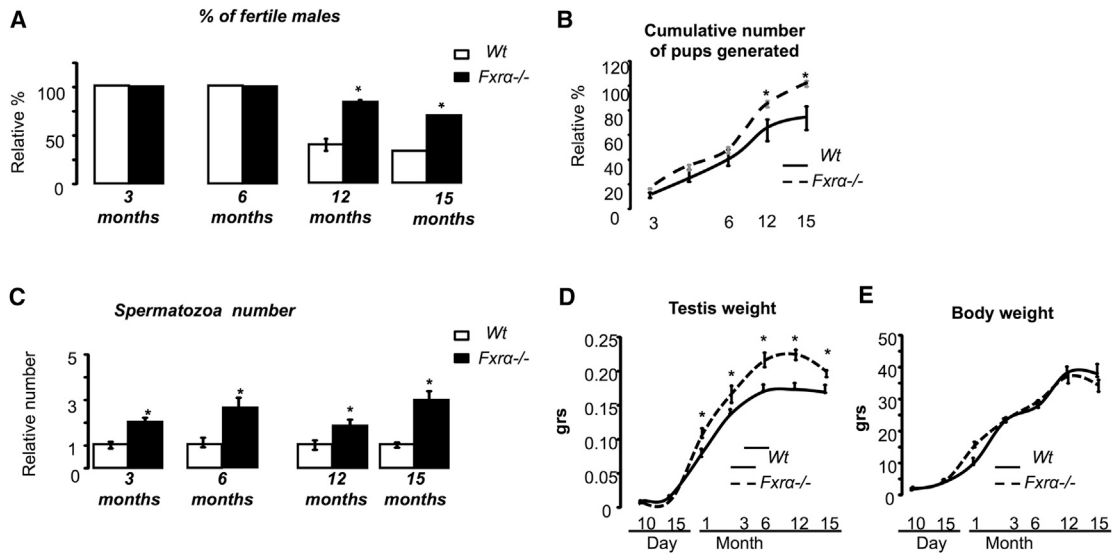

Figure 1. Lack of Fxrα Affects Fertility and Germ Cell Homeostasis

(A) Analysis of the percentages of fertile *wild-type* (WT) or *Fxrα*$^{-/-}$ males at 3, 6, 12, or 15 months of age.

(B) Cumulative number of pups obtained for *WT* and *Fxrα*$^{-/-}$ males of 3, 6, 12, or 15 months old.

(C) Relative spermatozoa count in the epididymis head in WT and *Fxrα*$^{-/-}$ at 3, 6, 12, or 15 months old. Wild-type were arbitrarily fixed at 1 as reference.

(D) Testis weight in *WT* and *Fxrα*$^{-/-}$ mice from 10 days post-natal (dpn), 15 dpn, 3 months, 6 months, 12 months, and 15 months old.

(E) Body weight of *WT* and *Fxrα*$^{-/-}$ mice of 10 dpn, 15 dpn, 3 months, 6 months, 12 months, and 15 months old.

Error bars indicate SEM. In all panels for each group, n = 10 males from three to four independent litters; *p < 0.05.

spermatozoa production is associated with a high number of promyelocytic leukemia zinc-finger protein (PLZF)-positive undifferentiated germ cells (UGCs) during aging. This points to involvement of FXRα in the control of germ cell fate. FXRα acts in part within the germ cell lineage, where it regulates the expression of several pluripotency factors such as the RNA-binding protein Lin28.

RESULTS

FXRα$^{-/-}$ Mice Maintain Reproductive Capacities throughout Aging

To analyze the impact of the nuclear receptor FXRα on testis physiology, we first analyzed the effects of FXRα deficiency (*Fxrα*$^{-/-}$) on fertility capacities in mice. As Fxrα is expressed in different cell types of the testis, we used a full-knockout model (Baptissart et al., 2016). During aging, more Fxrα$^{-/-}$ males remained fertile than wild-type (WT) (Figure 1A). *Fxrα*$^{-/-}$ males generated a higher cumulative number of pups than WT males during aging (Figure 1B). This was correlated with a greater production of spermatozoa by the *Fxrα*$^{-/-}$ mice as revealed by counting the number of spermatozoa in the head of the epididymis from 3 months of age. Interestingly, this difference was still observed at age 12 and 15 months (Figure 1C). A higher testis weight was observed in *Fxrα*$^{-/-}$ mice than in WT males from 3 to 15 months of age (Figure 1D). The higher sperm numbers in *Fxrα*$^{-/-}$ mice were still observed even when normalized to testis weight (Figure S1A). No difference was observed in body weight between genotypes at any of the ages analyzed (Figure 1E).

Lack of FXRα Alters the Post-natal Testicular Histology

Fertility results in part from intact testicular physiology enabling spermatozoa production. The establishment of testis physiology is a long-term developmental process starting at the fetal stage and continuing throughout the post-natal period. Here different testis weight was observed between *Fxrα*$^{-/-}$ and *WT* males from age 1 month (Figure 1D) but with no major difference in body weight (Figure 1E). Throughout life, no major abnormalities of testicular histology were observed (Figure S1C). However, analysis of testicular histology at a time point (15 days post-natal [dpn]) (see Figures S1B and S1C) when testis weight was not different between genotypes showed the impact of FXRα deficiency (Figure 2). Indeed, histological analyses showed abnormalities of the seminiferous epithelium from 15 dpn. H&E approaches demonstrated a greater number of seminiferous tubules without an open lumen in *Fxrα*$^{-/-}$ males than in WT males at 15 dpn (Figures 2A and

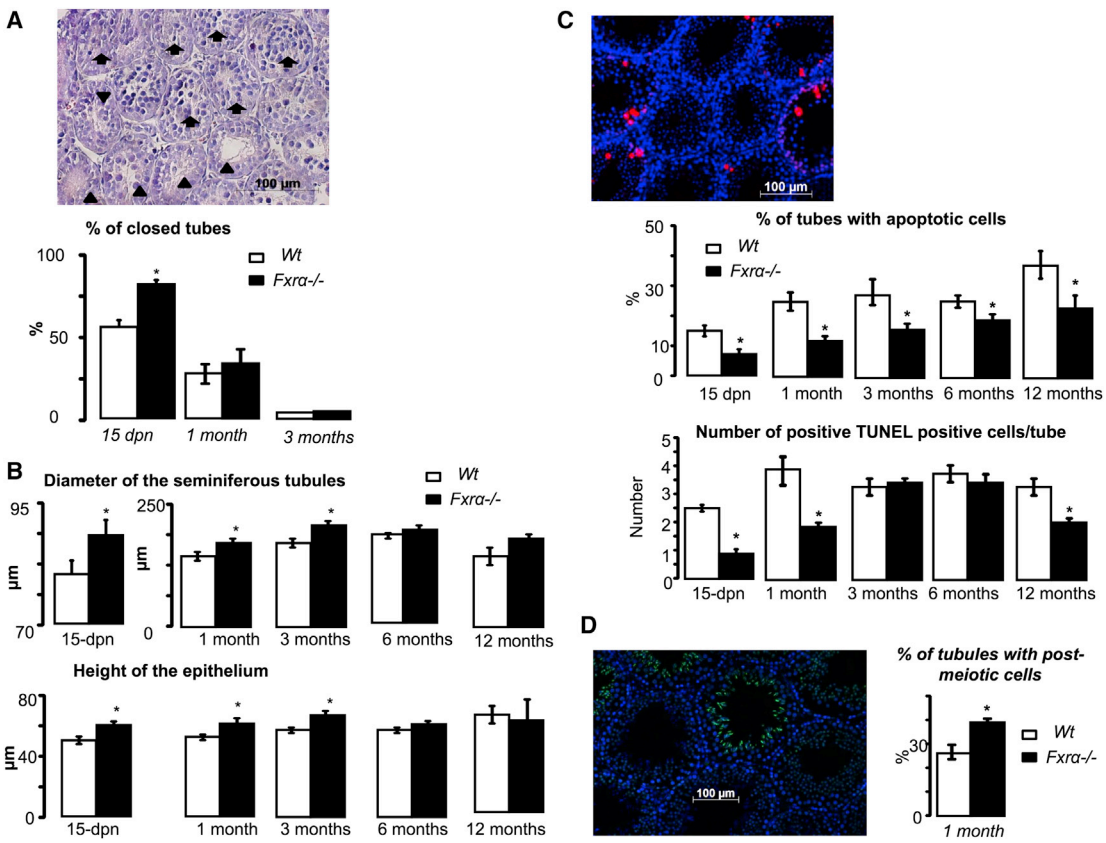

Figure 2. Lack of Fxrα Alters Testis Histology

(A) Representative micrograph of an *Fxrα*$^{-/-}$ testis of at 15 dpn. Arrows indicate closed seminiferous tubules, and arrowheads indicate seminiferous tubules with open lumen. Quantification of the percentage of tubules with closed lumen per 100 seminiferous tubules.

(B) Evaluation of the seminiferous tubule diameter (TD) and the epithelium height (EH) in *WT* and *Fxrα*$^{-/-}$ mice from 15 dpn to 12 months of age.

(C) Representative micrograph of a TUNEL-stained testis. Quantification of the number of TUNEL-positive seminiferous tubules and the number of TUNEL-positive spermatocytes are indicated as the number of positive seminiferous tubules or cells per 100 seminiferous tubules in *WT* and *Fxrα*$^{-/-}$ mice from 15 dpn to 12 months of age.

(D) Representative micrograph of a testis of 1-month-old *Fxrα*$^{-/-}$ male stained with acetylated H4. The original magnification was ×200. Quantification of the percentage of seminiferous tubules showing elongated H4ac-positive germ cells in *WT* and *Fxrα*$^{-/-}$ mice at 1 month of age.

Error bars indicate SEM. In all panels for each group, n = 10 males from three to four independent litters; *p < 0.05.

S1B). This delay in testicular development was transient; the difference in the opening of seminiferous tubules was no longer observed at ages 1 or 3 months (Figure 2A). As there was no longer any difference between genotypes, this parameter was not analyzed in older mice (ages 6 and 12 months).

In addition, the diameter of the seminiferous tubule was larger in *Fxrα*$^{-/-}$ males than in WT from 15 dpn (Figures 2B and S1B). In addition, the epithelium height was thicker in *Fxrα*$^{-/-}$ males than in WT males from 15 dpn to 3 months (Figures 2B and S1B). Taken together, these data suggest that *Fxrα* deficiency led to an earlier establishment of spermatogenesis during early post-natal development.

Interestingly, TUNEL analyses showed that from 15 dpn to 12 months of age, FXRα deficiency was associated with a lower apoptotic rate in the testis (Figure 2C).

Lack of FXRα Impairs Sertoli Cell Functions

The structure of the seminiferous epithelium is dependent on Sertoli cell functions. The number of Sertoli cells was higher in Fxrα$^{-/-}$ males at 10 dpn than in WT, but was no longer different at 15 dpn between genotypes, as supported by immunohistochemistry experiments (Figure S2A). At this time point of development, the Sertoli cells had their expected localization at the periphery of the tubules (Figure S2B). In addition, no alteration of the

proliferation status of Sertoli cells was observed between WT and Fxrα$^{-/-}$ males (Figure S2B). This time of development (15 dpn) also corresponds to the establishment of a functional blood-testis barrier (BTB). No difference was observed between genotypes in the efficiency of the BTB (Figure S2C). A lower number of Sertoli cells was observed in *Fxrα*$^{-/-}$ mice than in WT males from 1 month up to 12 months of age, as evaluated by the number of SOX9-positive cells per seminiferous tubule (Figure S2A). This reduction in the number of Sertoli cells was confirmed at the molecular level, with a lower accumulation of mRNA of specific Sertoli cell markers such as *Osp, Amh, Fshr,* and *Inhbb* (Figure S2D).

Lack of FXRα Affects Leydig Cell Function

Sertoli cells have been clearly shown to be dependent on the androgen status resulting from Leydig cell activity. *Fxrα* activation has been described as repressing the endocrine function of the testis. We thus analyzed the endocrine status of WT and *Fxrα*$^{-/-}$ mice from 15 dpn when the Sertoli cells showed altered transcriptome independent of effects on their number. The *Fxrα*$^{-/-}$ males showed lower intratesticular testosterone levels at 15 dpn to 3 months of age (Figure S3A). These results were supported by a lower testicular mRNA accumulation of genes involved in steroidogenesis such as *Cyp11a1* and *3β-hsd* (Figure S3B). The significance of this regulation was also emphasized by a lower mRNA accumulation of genes defined as androgen dependent, such as *Pem, Osp, Pci,* and *Tsx* (Figure S4A). This effect was intrinsic to Leydig cells, as a lower synthesis of testosterone was observed in a primary culture of *Fxrα*$^{-/-}$ Leydig cells than in WT cultures (Figure S4B). Such repression of steroidogenesis by Fxrα deficiency was surprising, as activation of FXRα by a synthetic agonist was also shown to repress testicular steroidogenesis via the induction of the expression of the small heterodimer partner (*Shp*; *Nr0b2*) (Baptissart et al., 2016) (Volle et al., 2007a). The fact that the same effects were observed on testosterone synthesis in conditions of activation of FXRα or of Fxrα deficiency could be explained, as the expression of *Shp* was found to be increased in the *Fxrα*$^{-/-}$ mouse compared with *WT* males (Figure S4C). The same increase in *Shp* mRNA accumulation was observed in primary cultures of *Fxrα*$^{-/-}$ Leydig cells compared to WT Leydig cells (Figure S4C). Interestingly, no difference in intratesticular levels was observed in older mice at ages 6, 12, and 15 months (Figure S3A). However, some impairments of the androgen signaling pathway could not be ruled out, as the mRNA accumulations of androgen-dependent genes were altered (Figure S4A).

These data suggest that testosterone homeostasis could be involved in the alterations of Sertoli cell homeostasis in Fxrα$^{-/-}$ males. However, this is not in line with the higher spermatozoa production in Fxrα$^{-/-}$ compared with WT males. This suggests that FXRα might control germ cell homeostasis independently of somatic testicular cells, namely Sertoli and Leydig cells.

Lack of FXRα Affects Functions of Germ Cell Physiology

The thicker epithelium of seminiferous epithelium from 15 dpn prompted us to analyze the status of spermatogenesis during early post-natal development. In mice, germ cells enter meiosis at around 10 dpn, and first post-meiotic cells can be observed at age 1 month. *Fxrα*$^{-/-}$ males had more seminiferous tubules with post-meiotic germ cells at 1 month than WT, as shown using immunostaining against the acetylated histone H4, which is specific to post-meiotic germ cells (Figures 2D and S5A). This was associated with a higher mRNA accumulation of specific markers of post-meiotic cells such as *Tnp1, Tnp2, Prm1,* and *Prm2* (Figure S5B). Interestingly, a higher mRNA accumulation of post-meiotic markers was still observed in *Fxrα*$^{-/-}$ males up to age 15 months (Figure S5B).

To determine whether the meiotic process could be altered (advanced) in *Fxrα*$^{-/-}$ males, we analyzed the expression of specific markers. Results showed that at 10 dpn, a time point compatible with the meiotic process of the first spermatogenic wave in the mouse, *Fxrα*$^{-/-}$ males expressed higher levels of meiotic genes such as *Stra8* and *Dmc1* (Figure 3A). These findings suggest that the retinoic pathway may be more active in *Fxrα*$^{-/-}$ males than in WT males. This is supported by the lower expression of retinoic acid (RA)-degrading enzyme *Cyp26b1* (Figure 3A). To verify the role of the RA pathway in the observed phenotype, we exposed *Fxrα*$^{-/-}$ males to a pan-RA receptor (pan-RAR) antagonist (AGN-194610) at 8 and 10 dpn. Exposure to AGN-194610 resulted at 25 dpn in a complete deletion of differentiating and differentiated germ cells as supported by histological analyses (Figure 3B): this resulted in an increased number of PLZF^{+} undifferentiated spermatogonia (Figure 3C). These findings are consistent with the observed earlier germ cell differentiation in 1-month-old *Fxrα*$^{-/-}$ males. Interestingly, the increased mRNA accumulation of meiotic genes was not further maintained in older mice (Figure S6A): older Fxrα$^{-/-}$ mice showed lower mRNA accumulation of these genes than WT (Figure S6A). This could reflect the dilution of meiotic genes in the testis producing a greater number of spermatozoa.

Regarding the impact of Fxrα deficiency on spermatogenesis during early post-natal development, we also analyzed undifferentiated spermatogonia: this cell population plays an important role, as it supports spermatogenesis from puberty to adulthood. We performed experiments on mice of both genotypes starting at 10 dpn, as this age corresponds to the time point when the pool of UGCs is established and

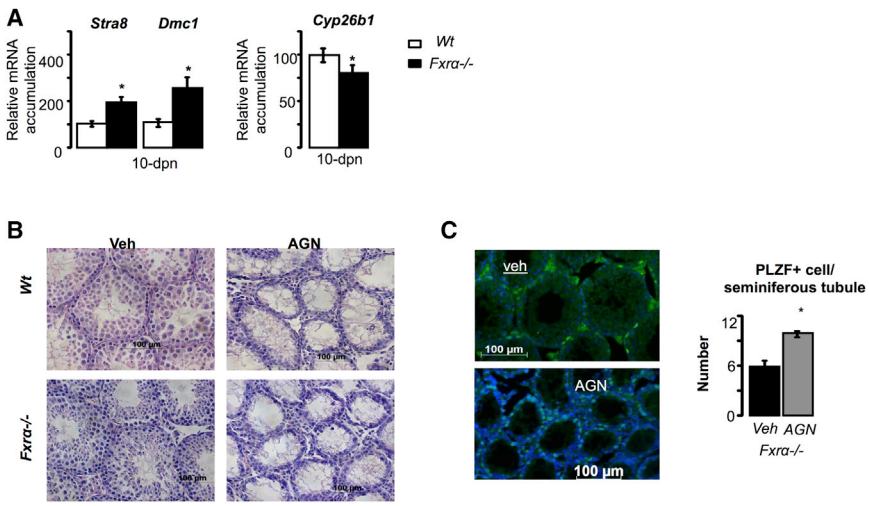

Figure 3. Lack of Fxrα Affects Meiosis Process

(A) Testicular mRNA accumulation of *Stra8, Dmc,* and *Cyp26b1* normalized to *β-actin* mRNA levels in *WT* and *Fxrα*$^{-/-}$ mice at 10 dpn. n = 5–10 per group; *p < 0.05.

(B) Representative micrographs of the testis of *WT* and *Fxrα*$^{-/-}$ mice treated with vehicle (DMSO) or AGN-191046 (a pan-RAR antagonist). The original magnification was ×200.

(C) (Left) Representative micrographs of the testis stained for PLZF from 25-dpn *Fxrα*$^{-/-}$ mice treated with vehicle (DMSO) or AGN (pan-RAR antagonist). The original magnification was ×200. (Right) Quantification of the relative number of PLZF-positive cells per seminiferous tubule 2 weeks after treatments. n = 5–10 per group; *p < 0.05. Error bars indicate SEM.

germ cells enter the first wave of spermatogenesis. Immunohistochemistry experiments showed more PLZF-positive cells per seminiferous tubule in *Fxrα*$^{-/-}$ males than in WT males from 10 dpn (Figure 4A). Interestingly, the results showed a greater number of PLZF-positive undifferentiated spermatogonia up to age 12 months (Figure 4A).

The establishment of the pool of UGCs results from a balance between proliferation and apoptosis. At 10 dpn, the increased number of PLZF-positive cells in Fxrα$^{-/-}$ males was not associated with a higher proliferation rate, the number of PLZF^{+}/proliferating cell nuclear antigen (PCNA)$^{+}$ cells within the seminiferous tubules being not different from that in WT males (Figure 4B). The analysis of co-stained PLZF/TUNEL cells demonstrated a lower apoptotic rate of PLZF cells at age 10 days (Figure 4C). The importance of the lower apoptotic rate in the establishment of a different number of PLZF^{+} cells in *Fxrα*$^{-/-}$ males was supported by the finding that when apoptosis was induced using busulfan (1 week; Figures S6B and 6C), the number of PLZF^{+} cells was normalized between WT and *Fxrα*$^{-/-}$ males (Figure 4D). In addition, an impact of *Fxrα* deficiency was observed on proliferation rate of PLZF^{+} cells only at ages 1 and 3 months, when a greater number of PCNA/PLZF cells was noted (Figure 4B), and a lower apoptotic level of PLZF was observed at 6 months and 12 months (Figure 4C). Taken together, these results suggest that a shift in the balance between proliferation and apoptosis could be in part responsible for the establishment of a greater number of UGCs in *Fxrα*$^{-/-}$ males than in *WT* males.

FXRα Controls Early Post-natal Molecular Signature of the Testis

The aforementioned results support the hypothesis that some intrinsic parameters of germ cells are modified in Fxrα deficiency. To better define how Fxrα affects the testis, particularly regarding the establishment of the number of UGCs, we used an RNA sequencing (RNA-seq) approach at 10 dpn when the germ cells/Sertoli cells ratio was not altered owing to the decrease in Sertoli cells in older animals (Figure 5). We found that in Fxrα$^{-/-}$ testis the mRNA accumulation of 3,453 genes was altered compared with WT animals, with 57% downregulated and 43% upregulated genes (Figure 5A and Table S1). Among the differentially expressed (DE) genes, some were enriched in particular cell types of the testis such as Leydig and Sertoli cells (Figure 5B). Consistent with the above findings, a comparison with specific genes, previously reported to be enriched in either Leydig or Sertoli cells (Sanz et al., 2013), showed that most of the genes expressed in these two cell types were repressed in Fxrα$^{-/-}$ compared with WT mice (Figure 5C) (the lists of genes with which the comparisons were made are given in Tables S2 and S3). Gene ontology analysis highlights clusters of developmental genes (Figure 5D). In the clusters of *Hox* or *Pou* genes, a high proportion showed an increased mRNA accumulation in Fxrα$^{-/-}$ testis (Figures 5E and 5F). Gene ontology analysis also reveals several clusters of altered genes related to reproduction and gametogenesis (Figure 5D).

Consistent with the lower apoptotic rate of germ cells at 15 dpn, the RNA-seq analysis of Fxrα$^{-/-}$ testis identified several genes known to be involved in germ cell apoptotic processes such as *Pxt1* (Kaczmarek et al., 2011), *Bak1* (Kratz et al., 2011), and *Caspase-6* (Omezzine et al., 2003), which were validated by qPCR analysis (Figure 6A). Caspase-6 protein accumulation was lower in *Fxrα*$^{-/-}$ than in WT males (Figure 6B). The mRNA accumulations of these genes were found to be decreased in *Fxrα*$^{-/-}$ males compared with WT aged up to 3 months (Figure S7A).

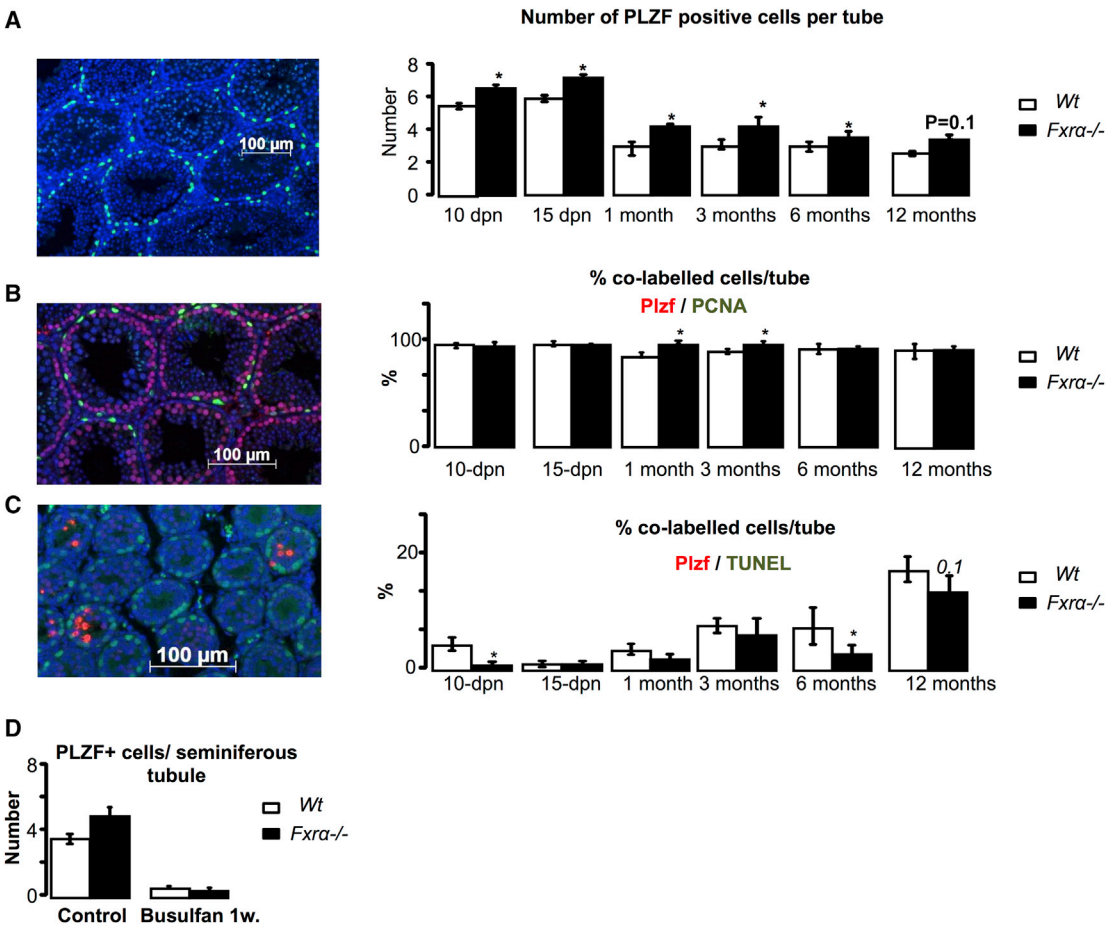

Figure 4. Lack of Fxrα Alters Germ Cells

(A) (Left) Representative micrograph of a *Fxrα*$^{-/-}$ testis stained for PLZF. The original magnification was ×200. (Right) Quantification of the relative number of PLZF-positive cells per seminiferous tubules at 10 dpn, 15 dpn, 1 month, 3 months, 6 months, 12 months, or 15 months old.

(B) (Left) Representative micrograph of a testis stained for PCNA and PLZF. The original magnification was ×200. (Right) Quantification of the relative number of positive cells for PLZF and PCNA per seminiferous tubule at 10 dpn, 15 dpn, 1 month, 3 months, 6 months, 12 months, or 15 months old.

(C) (Left) Representative micrograph of a testis stained for TUNEL. The original magnification was ×200. (Right) Quantification of the relative number of positive cells for PLZF and TUNEL per seminiferous tubule at 10 dpn, 15 dpn, 1 month, 3 months, 6 months, 12 months, or 15 months old.

(D) Quantification of the relative number of PLZF-positive cells per seminiferous tubule 1 week after busulfan treatment.

Error bars indicate SEM. In (A), (B), and (C), for each group n = 10 males from three to four independent litters; *p < 0.05. In (D) and (E), for each group n = 8 males from four independent litters; *p < 0.05.

To explain the maintenance of the reproductive capacities of Fxrα$^{-/-}$ males during aging, we focused on genes expressed in spermatogonia, as these cells ensure the initiation of spermatogenesis and the maintenance of germ cell lineage through UGCs. We compared the RNA-seq data with a specific list of genes known to be expressed in spermatogonia (Table S4) (Chan et al., 2014; Delbès et al., 2004; Hammoud et al., 2009; Iwamori et al., 2013; Mu et al., 2014). Among these 60 genes, 30% were statistically deregulated in Fxrα$^{-/-}$ males, with 13 upregulated and 5 downregulated genes (Figure 6C). Among the upregulated genes, some were associated with UGCs such as *Pou5f1, Nanog,* or *Thy1*, while others indicated pro-differentiating germ cells such as *Sohlh2* and *Sohlh1*, and decreased *Pak6* expression. This suggests that FXRα regulates germ cell fate through maintenance of UGCs and/or regulation of germ cell differentiation (Figures 6C and 6D). On the other hand, at 10 dpn, qPCR experiments confirmed that Fxrα$^{-/-}$ males had a higher expression of cell type markers such as *Pou5f1, Nanog,* and *Lin28*

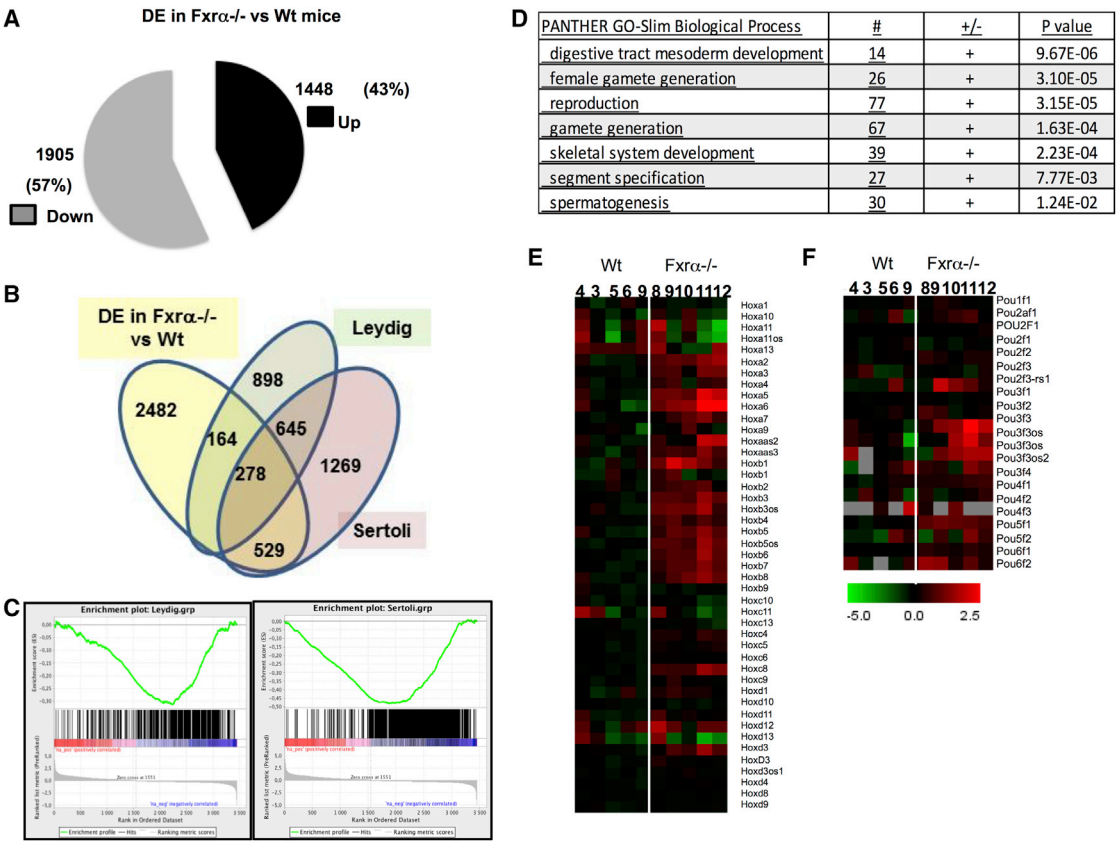

PANTHER GO-Slim Biological Process	#	+/-	P value
digestive tract mesoderm development	14	+	9.67E-06
female gamete generation	26	+	3.10E-05
reproduction	77	+	3.15E-05
gamete generation	67	+	1.63E-04
skeletal system development	39	+	2.23E-04
segment specification	27	+	7.77E-03
spermatogenesis	30	+	1.24E-02

Figure 5. Lack of Fxrα Alters Early Post-natal Testis Transcriptome

(A) Analysis of differentially expressed genes (DE) in WT versus FXRα$^{-/-}$ testis at 10 dpn.

(B) Venn diagram for DE genes in WT versus FXRα$^{-/-}$ and specifically compared with Leydig- or Sertoli-cell-enriched genes.

(C) GSEA analysis comparing DE genes in WT versus FXRα$^{-/-}$ with specific enriched genes in Leydig or Sertoli cells from Sanz et al. (2013) (see Tables S2 and S3).

(D) Gene ontology analysis on DE genes in WT versus FXRα$^{-/-}$.

(E) Specific heatmap for Hox and Pou clusters in DE genes in WT versus FXRα$^{-/-}$.

Error bars indicate SEM. In all panels, for each group n = 5 males from three independent litters.

(Figure 6E), suggesting a greater number of undifferentiated spermatogonia.

To determine how FXRα deficiency led to an increase in the number and maintenance of UGCs, in addition to *Oct3/4, Nanog,* and *Thy1* we also focused on the altered expression of several genes known to play roles in the homeostasis of undifferentiated germ cells such as *Lin28* (West et al., 2009; Zheng et al., 2009), *Erβ* (*Ers2*) (Delbès et al., 2004), and *Jmjd3* (*Kdm6b*) (Iwamori et al., 2013). Interestingly, *Lin28, Erβ,* and *Jmjd3* mRNA accumulations were altered in Fxrα$^{-/-}$ males compared with WT animals as observed in RNA-seq data and/or qPCR validation experiments (Figures 6C–6E).

FXRα Acts in Germ Cells

To determine whether the lack of Fxrα on the expression of these genes could directly affect germ cells, we analyzed the Fxrα expression profile. Ontogeny analyses showed that in early post-natal development, when the pool of UGCs is established, the expression pattern of *Fxrα* was similar to the early germ cell marker G9a (EMHT2) (Figure 7A). In addition, we studied the expression of *Fxrα* in the mouse spermatogonial cell line GC-1spg. The expression of Fxrα in this cell line was validated using a specific small interfering RNA (siRNA) directed against Fxrα (Figure 7B). The efficiency of FXRα activation by the GW4064 in GC1spg was proved by the increased expression of *Shp*, a known FXRα target gene (Figure 7C). Taken together, these data support the expression of Fxrα in germ cells. We thus analyzed the impact of specific siRNA directed against *Fxrα* (*si-Fxrα*) in the spermatogonial germ cell line GC1-spg. Unfortunately, we were unable to detect any expression of *Oct3/4, Nanog*, or *Erβ* in the GC1-spg cell line. No effect of the si-FXRα was

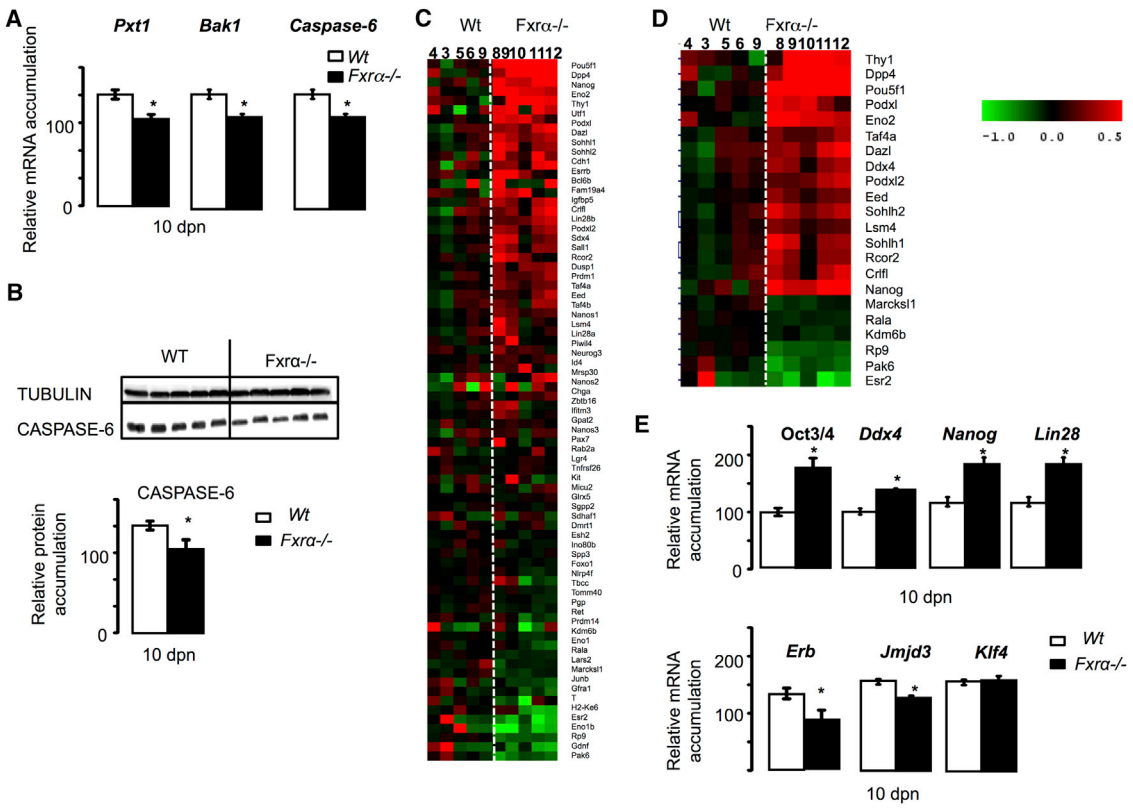

Figure 6. The Lack of FXRα Alters Spermatogenesis Process

(A) Testicular mRNA accumulation of *Pxt1*, *Bak1*, and *Caspase-6* normalized to *β-actin* mRNA levels in testes of 15-day-old WT and Fxrα$^{-/-}$ mice.

(B) Representative western blots of CASPASE-6 and TUBULIN, and quantification of the CASPASE-6/TUBULIN ratio in testis of WT and Fxrα$^{-/-}$ testis at 15 dpn.

(C) Heatmap analysis of DE genes in WT versus FXRα$^{-/-}$ and specifically compared with germ cell-enriched genes (Table S4).

(D) Heatmap analysis of statistically significant DE genes in WT versus FXRα$^{-/-}$ and specifically compared with germ cell-enriched genes (Table S4).

(E) Testicular mRNA accumulation of *Oct3/4*, *Ddx4*, *Nanog*, *Lin28*, *Erβ*, *Klf4*, and *Jmjd3* normalized to *β-actin* mRNA levels in 10-day-old *WT* and *Fxrα*$^{-/-}$ mice.

Error bars indicate SEM. In (A), (B), and (E), for each group n = 6–10 males from four to five independent litters; *p < 0.05. In (C) and (D), for each group n = 5 males from three independent litters.

observed on *Jmjd3* mRNA accumulation (Figure 7D). Consistent with data obtained in the *Fxrα*$^{-/-}$ males, *Lin28* mRNA accumulation was increased in cells transfected with the si-Fxrα compared with siRNA-control (*si-Ctrl*) conditions (Figure 7D). To better define how FXRα controls *Lin28* expression, we analyzed the impact of FXRα activation by synthetic agonist GW4064 in the germ cell lineage using the GC1-spg cell line. Lin28 mRNA accumulation decreased in response to GW4064 exposure (Figure 7E).

Analysis of putative target genes of LIN28 against the list established as common targets for *Pou5f1* and *Nanog* in human embryonic stem cells (Hosseinpour et al., 2013; Park et al., 2012) revealed that in the testicular RNA-seq data some of them were specifically altered in Fxrα$^{-/-}$ males compared with *WT* males (Figure 7F) with 50% upregulated (Pou5f1; Nanog, Utf1) and 50% downregulated (Tiam1, Cdh2).

These findings suggest either that *Lin28* is a direct target gene of FXRα through a negative response element (hypothesis 1, Figure 7G), as shown for apolipoprotein A1 (Claudel et al., 2002) or, as no classical FXRE was identified using Genomatix on mouse Lin28 5′-flanking sequences, that FXRα acts through an indirect mechanism (hypothesis 2, Figure 7G). Among the different factors known to regulate *Lin28* expression, as identified in the RNA-seq data, none were deregulated, at least not so as to explain the upregulation of Lin28 in the Fxrα$^{-/-}$ testis (Figure 7G).

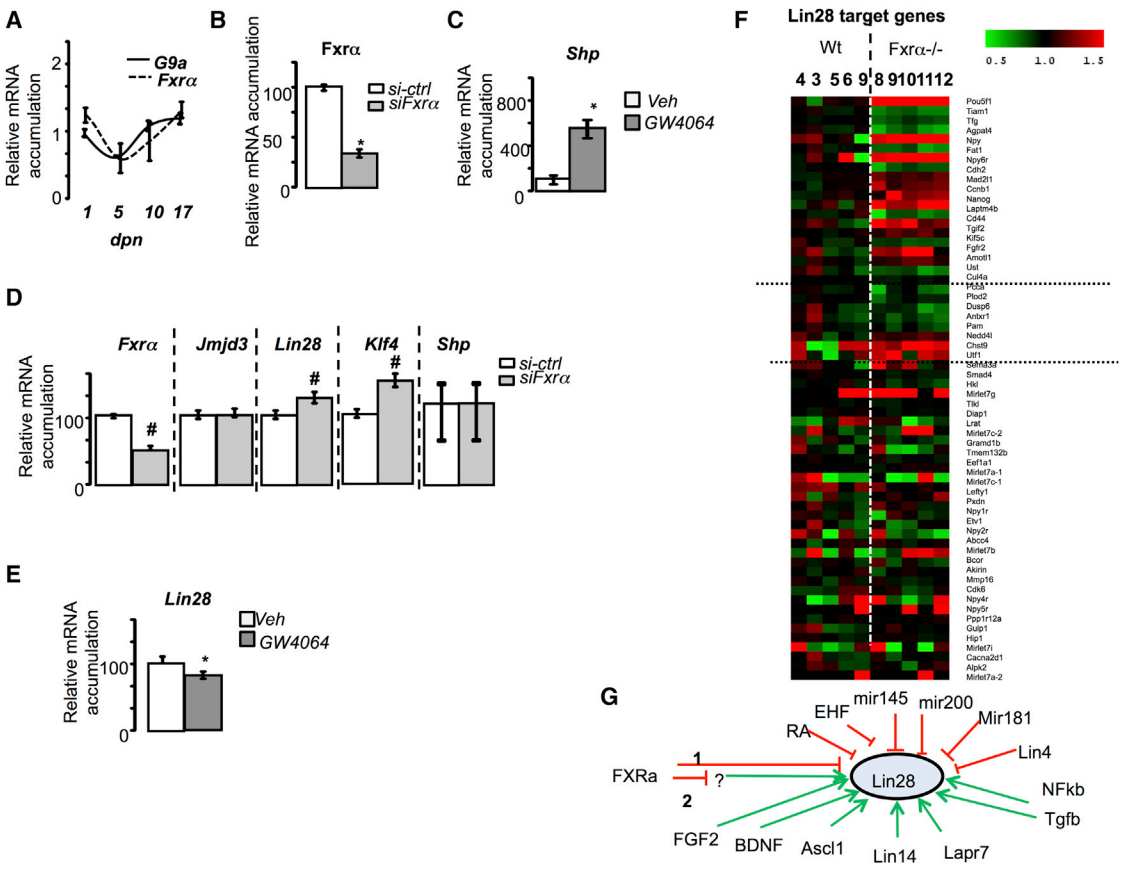

Figure 7. FXRα Acts in Germ Cell Lineage

(A) Testicular mRNA accumulation of *G9a* and *Fxrα* normalized to β-actin mRNA levels in whole testes of C57BL/6J at 1, 5, 10, and 17 dpn.

(B) Relative Fxrα mRNA accumulation normalized to β-actin in GC-1spg cells transfected with control siRNA or siRNA directed against Fxr.

(C) mRNA accumulation of *Shp* normalized to *β-actin* mRNA levels in GC1spg cells treated with DMSO or GW4064 (10^{-6} M).

(D) Relative *Fxrα, Jmjd3, Lin28, Klf4,* and *Shp* mRNA accumulation normalized to β-actin.

(E) mRNA accumulation of *Lin28* normalized to *β-actin* mRNA levels in GC1spg cells treated with DMSO or GW4064 (10^{-6} M).

(F) Heatmap analysis of Lin28 target genes in WT versus *Fxrα*$^{-/-}$ in RNA-seq dataset.

(G) Schematic model representing the known regulators of *Lin28* expression.

Error bars indicate SEM. In (A), for each group n = 6 males from four independent litters. In (B) to (E), the data originate from four independent experiments with triplicates per group for each experiment. *$p < 0.05$, #$p < 0.01$. In (F), for each group n = 5 males from three independent litters.

DISCUSSION

FXRα was initially shown to regulate the enterohepatic cycle and BA biosynthesis. In recent decades, many studies have demonstrated its involvement in other physiological functions (digestion, immunity) and diseases such as diabetes and cancer. FXRα participates in the homeostasis of steroids through the control of their synthesis and/or catabolism (Baptissart et al., 2013). To date, in the testis FXRα has been shown to be expressed in Leydig cells where it controls testicular testosterone metabolism. However, its effects on the exocrine function have not yet been explored. Here we identified unexpected roles of FXRα in testis physiology, mainly in the germ cell lineage.

FXRα Deficiency Reveals Intrinsic Germ Cell Capacities Independent of Leydig and Sertoli Cell Functions

Our findings clearly show that lack of FXRα altered Leydig and Sertoli cell physiologies. However, the most striking results were on germ cells, supporting the existence of intrinsic roles of FXRα in the germ cell lineage.

We demonstrate that FXRα participates in the control of germ cell survival through a mechanism independent of androgen status, at least in young mice. At the molecular

level, the androgen independency of germ cells in Fxrα$^{-/-}$ males is consistent with the regulation of *caspase-6* by FXRα. Furthermore, in the liver the bile acid-induced apoptosis is dependent on CASPASE-6 (Rust et al., 2009). In addition, a previous study using anti-androgen treatment has demonstrated that caspase-6 is a critical actor of the apoptosis induced in response to low androgen concentrations (Omezzine et al., 2003).

Other results support the finding that FXRα signaling pathways affect germ cell physiology: Fxrα$^{-/-}$ males showed a high production of spermatozoa even in a context of lower Sertoli cell numbers and an altered Sertoli transcriptome. Sertoli cells have been shown to be important for germ cell differentiation: the present results will help to better define the key Sertoli cell factors that are essential to support spermatogenesis.

Our results suggest that intrinsic germ cell pathways targeted by FXRα exist to efficiently sustain full spermatogenesis even in a relatively autonomous manner.

Interestingly, an early entry into meiosis was noted in the *Fxrα*$^{-/-}$ males compared with *WT* males. Although this pathway was not fully studied in the present work, these phenomena may be associated with the modulation of the retinoid pathway, as some key target genes of retinoids were upregulated in *Fxrα*$^{-/-}$ males, such as *Stra8*. This early activity of the retinoid could be correlated with the lower expression of retinoid-degrading enzyme *Cyp26b1* in Fxrα knockout mice compared with WT males. These findings were supported by the use of a pan-antagonist of RAR, which completely blocked germ cell differentiation in both WT and Fxrα$^{-/-}$ males.

FXRα and the Establishment and Maintenance of Undifferentiated Germ Cells

The pool of SSCs is established early after birth by gonocytes. Our understanding of how the SSC pool is established has progressed in the last few years. However, the population of undifferentiated spermatogonia is heterogeneous, hindering the identification of specific markers. Besides these markers, there is also a need to better define the mechanisms involved in regulating the establishment of the UGC population. Fxrα$^{-/-}$ males maintained a greater number of undifferentiated germ cells (PLZF^{+}) than WT throughout aging. Only SSCs have regenerative capacity and sustain spermatogenesis, whereas progenitors lack this regenerative capacity. Here we demonstrate that aged Fxrα$^{-/-}$ males maintained fertility capacities comparable with those of young animals. This supports the hypothesis that FXRα participates in the establishment and maintenance of a pool of SSCs. Furthermore, we demonstrate that the expression of *Jmjd3* was decreased in *Fxrα*$^{-/-}$ males. It was recently demonstrated that mice invalidated for the gene encoding *Jmjd3* in germ cells had heavier testes and maintained reproductive capacities for longer than WT littermates (Iwamori et al., 2013). This phenotype is quite similar to that of *Fxrα*$^{-/-}$ mice. This suggests that the decreased expression of *Jmjd3* might be involved in the maintained fertility in *Fxrα*$^{-/-}$ males compared with *WT*.

At the molecular level, several testicular target genes of FXRα in vivo may be related to the establishment of the number of SSCs. Among the genes studied, we identified altered expression of *Oct3/4, Nanog, Lin28,* and *Erβ* in the *Fxrα*$^{-/-}$ males compared with *WT*. The post-natal establishment of the number of gonocytes was previously shown to increase in the context of *Erβ* (*Ers2*) deficiency (Delbès et al., 2004). This phenotype is associated with an increase in proliferation and a decrease in the apoptotic process of germ cells. This is close to the phenotype observed in early post-natal Fxrα$^{-/-}$ males. Consistent with this, *Erβ* was decreased in Fxrα$^{-/-}$ males.

Lin28 was altered by exposure to the agonist or by invalidation of FXRα. Lin28 thus appears to be a good candidate to explain part of this phenotype. Lin28 is critical for the development of primordial germ cells, and marks undifferentiated spermatogonia in mice throughout their lifetimes (West et al., 2009; Zheng et al., 2009). Moreover, lower expression of *Lin28* has been demonstrated to affect the expression of *Oct3/4, Nanog,* or *Utf1*. Thus its higher expression in response to FXRα signaling pathways is consistent with the observed modulation of these pluripotency genes. This supports the hypothesis that Lin28 is a mediator of the FXRα effect on pluripotency and homeostasis of germ cells (Figure S7B).

Interestingly, *Lin28* was oppositely affected by FXRα activation or invalidation, suggesting that Lin28 could be a direct gene of FXRα through a negative response element (hypothesis 1, Figure 7G) as shown for apolipoprotein A1 (Claudel et al., 2002). However, no classical FXRE was identified using Genomatix on mouse Lin28 5′-flanking sequences. It could thus also be hypothesized that there is an indirect mechanism (hypothesis 2, Figure 7G) whereby FXRα controls the expression of a positive regulator of Lin28. Among the different factors known to regulate *Lin28* expression (Figure 7G), none were affected, at least not relevantly, in Fxrα$^{-/-}$ testis as identified in the RNA-seq data. Thus the exact mechanisms by which FXRα controls the expression of *Lin28* remain to be defined.

From a translational point of view, our results offer perspectives: in the last few years, progress has been made in in vitro spermatogenesis methods to circumvent the problem of azoospermic men excluded from procedures of microsurgical testicular sperm extraction, intracytoplasmic sperm injection, and round spermatid injection. Our results could be of interest in this context, where modulation of FXRα could both improve the maintenance of stem cells

and be beneficial for the progression into the differentiating steps (Figure S7B).

Our findings also open an area of research on the roles of FXRα in cellular homeostasis: whereas FXRα was previously known for controlling the differentiation process in adipocytes or bone marrow (Id Boufker et al., 2011; Rizzo et al., 2006), to our knowledge no data had yet been reported demonstrating the involvement of FXRα in stem cell fate. Our work could thus be extended to the intestine, liver, or other organs where FXRα plays major roles. Our findings open up important perspectives on many fields of research with potential impacts on major human health problems such as developmental abnormalities, metabolic diseases, cancer, and aging disorders.

EXPERIMENTAL PROCEDURES

Ethics Statement

This study was conducted in accordance with the current regulations and standards approved by the Animal Care Committee (C2E2A; protocol CE 07-12).

Animals

FXRα$^{-/-}$ mice used have been previously described (Baptissart et al., 2014) (Milona et al., 2010), and were in a C576Bl6 genetic background. Mice used in this study were maintained and housed in temperature-controlled rooms with 12-hr light/dark cycles. Mice had ad libitum access to food and water. Nine-week-old mice were fed 2016 rodent diet (Harlan).

For in vivo experiments, males were treated from birth and up to 15 dpn with vehicle (DMSO) or GW4064 (20 mg/kg/day) with an injection volume of 10 μL.

For busulfan experiments, mice were treated intraperitoneally with 20 mg/kg busulfan or vehicle (DMSO).

For anti-retinoid experiments, 8-day-old mice were treated intraperitoneally with 5 mg/kg AGN-194610 or vehicle (DMSO) at 8 and 10 dpn and were euthanized at 25dpn.

Fertility Test

Fifteen days before euthanasia each male was put into reproduction at night with two C57Bl6J females (Charles River) (4–5 males per group per experiment). Breeding was monitored daily for the presence of a vaginal plug to determine whether mating occurred. After 19–20 days, efficacy of mating was visually inspected by the female delivery and the number of pups per litter was counted.

Histology

The testes were collected, fixed in Bouin's solution or formalin and embedded in paraffin, and 5-μm-thick sections were prepared and stained with H&E (n = 6–10 animals per group).

For the analysis of the BTB integrity, an intratesticular injection of EZ-Link sulfo-NHS-LC-biotin (15 μL; 7.5 mg/mL) was performed intraperitoneally (Baptissart et al., 2014). The testes were harvested 30 min after injection, fixed in Bouin's solution and embedded in paraffin, and sections of 5 μm thickness were prepared.

TUNEL Analysis

TUNEL experiments were performed as previously described (Volle et al., 2007b) on 5 μm of testis fixed in Bouin's solution or paraformaldehyde 4%. In each testis, at least 100 random seminiferous tubules were counted. The results are expressed as the number of tubules with either spermatocytes or spermatids TUNEL positive per 100 seminiferous tubules.

Immunohistochemistry

Paraffin sections of testes fixed with Bouin's solution were sectioned at 5 μm. The sections were mounted on positively charged glass slides (Superfrost plus), deparaffinized, rehydrated, treated for 20 min at 93°–98°C in 0.01 M citric buffer (pH 6), rinsed in osmosed water (2 × 5 min), and washed (2 × 5 min) in Tris-buffered saline (TBS). Immunohistochemical studies were conducted according to the manufacturer's recommendations, as described earlier (Volle et al., 2009). Slides were then counterstained with Hoechst medium (1 mg/mL). The antibodies used were Sox9 (Millipore, AB535 [Maqdasy et al., 2015]) PCNA (Santa Cruz Biotechnology, Sc22839 [Volle et al., 2009]), and PLZF (Santa Cruz, sc56 [Gely-Pernot et al., 2015]).

Endocrine Investigations

Testosterone concentrations were measured from frozen testis extracted with 10 volumes of ethylacetate-isooctane (30:70, v/v) as previously described (Volle et al., 2007b). Intratesticular testosterone levels were measured using a commercial ELISA kit (Diagnostic Biochem).

Real-Time RT-PCR

RNA from testis samples was isolated using Nucleospin RNA L (Macherey Nagel). cDNA was synthesized from total RNA with the MMLV reverse transcriptase and random hexamer primers (Promega). Real-time PCR measurement of individual cDNAs was performed using SYBR green dye (Master mix Plus for SYBR Assay; Eurogentec) to measure duplex DNA formation with the Eppendorf Realplex system. The sequences of primers are given elsewhere (Baptissart et al., 2014; Vega et al., 2015; Volle et al., 2007b, 2007a, 2009). Standard curves were generated with pools of testis cDNA from animals with different genotypes and/or treatments. The results were analyzed using the ΔΔCt method.

RNA-Seq

The RNA-seq experiment was performed on testis of WT and *Fxrα*$^{-/-}$ mice at 10 dpn. Starting from RNA, all preparations were made using the IGBMC platform (Illkirch). The mRNA-seq libraries were sequenced (1 × 50 b).

Reads were mapped onto the mm10 assembly of the mouse genome using TopHat v2.0.10 (Kim et al., 2013) and the Bowtie2 v2.1.0 aligner (Langmead and Salzberg, 2012). Only uniquely aligned reads were retained for further analysis.

Quantification of gene expression was performed using HTSeq v0.5.4p3 (Anders et al., 2015) using gene annotations from Ensembl release 77.

Read counts were normalized across libraries with the method proposed by Anders and Huber (2010). Comparison between FXRα$^{-/-}$ and WT samples was performed using the method

proposed by Love et al. (2014) implemented in the DESeq2 Bioconductor library (DESeq2 v1.0.19). Resulting p values were adjusted for multiple testing using the method of Benjamini and Hochberg (1995). Raw data are available at GEO: GSE84945; datasets are available in Table S1.

Western Blot

Proteins were extracted from tissues using lysis buffer (0.4 M NaCl, 20 mM HEPES, 1.5 mM $MgCl_2$, 0.2 mM EDTA, 0.1% NP-40, 1× protease inhibitors [Roche Diagnostics]). Antibodies were used in TBS, 0.1% Tween, and 10% milk. The antibodies used are α-TUBULIN (Sigma-Aldrich, B512) and CASPASE-6 (Cell Signaling Technology, #9762).

Cell Studies

GC1-spg cells were used as previously described (Baptissart et al., 2014). Cells were treated for 24 hr with vehicle (DMSO, 1:1,000) or 10^{-6} M GW4064 (Sigma-Aldrich). Cells were then harvested 4 hr later, and mRNA or protein extractions were performed. The data presented were obtained from four independent experiments with n = 3 per group per experiment.

Transient Transfection

GC1-spg cells were transfected with siRNA using interferin (Ozyme) in 6-well plates (100,000 cells per well). The siRNA directed against *Fxrα* and control siRNA (siGfp) were transfected at 5 ng per well; 48 hr after the transfection, cells were treated for 12 hr with vehicle (DMSO, 1:10,000) or GW4064 (10^{-6} M). Cells were then harvested 64 hr later, and mRNA extractions performed. The data presented were obtained from four independent experiments with n = 3 per group per experiment.

Statistical Analyses

Number and type of replicates (e.g., technical replicates, independent experiment, number of mice, and number of independent litters) are reported in the figure legends. Error bars represent SEM, and statistical tests are described in the Experimental Procedures or legends. For all key experiments t tests were done and significance levels reported.

ACCESSION NUMBERS

The accession number for the RNA-seq data reported in this paper is GEO: GSE84945.

SUPPLEMENTAL INFORMATION

Supplemental Information includes seven figures and four tables and can be found with this article online at http://dx.doi.org/10.1016/j.stemcr.2017.05.036.

AUTHOR CONTRIBUTIONS

E.M., L.S., M.B., H.H., B.R., C.D.-S., A.D.H., J.-P.S., C.T., C.K., and D.H.V. performed the experiments. C.T., C.K., and G.B. analyzed the RNA-seq data. E.M. and D.H.V. designed experiments, and J.-M.A.L., S.B., F.C., C.B., and D.H.V. wrote the manuscript.

ACKNOWLEDGMENTS

This work was funded by Inserm, CNRS, Clermont Université, Ministère de l'Enseignement Supérieur et de la recherche (to M.B.), Ligue contre le Cancer (Comité Puy de Dôme to D.H.V.), Nouveau Chercheur Auvergne (no. R12087CC to D.H.V.), ANR Jeune Chercheur (no. 1103 to D.H.V.), and Plan Cancer – Cancer-Environnement InCa/Inserm (C14012CS to D.H.V.). We also thank Anipath platform from the GReD and the animal house staff (Sandrine Plantade, Philippe Mazuel, and Khirredine Ouchen).

Received: November 4, 2016
Revised: May 31, 2017
Accepted: May 31, 2017
Published: June 29, 2017

REFERENCES

Anders, S., and Huber, W. (2010). Differential expression analysis for sequence count data. Genome Biol. *11*, R106.

Anders, S., Pyl, P.T., and Huber, W. (2015). HTSeq—a Python framework to work with high-throughput sequencing data. Bioinformatics *31*, 166–169.

Baptissart, M., Vega, A., Martinot, E., Baron, S., Lobaccaro, J.M.A., and Volle, D.H. (2013). Farnesoid X receptor alpha: a molecular link between bile acids and steroid signaling? Cell. Mol. Life Sci. *70*, 4511–4526.

Baptissart, M., Vega, A., Martinot, E., Pommier, A.J., Houten, S.M., Marceau, G., de Haze, A., Baron, S., Schoonjans, K., Lobaccaro, J.M.A., et al. (2014). Bile acids alter male fertility through G-protein-coupled bile acid receptor 1 signaling pathways in mice. Hepatology *60*, 1054–1065.

Baptissart, M., Martinot, E., Vega, A., Sédes, L., Rouaisnel, B., de Haze, A., Baron, S., Schoonjans, K., Caira, F., and Volle, D.H. (2016). Bile acid-FXRα pathways regulate male sexual maturation in mice. Oncotarget *7*, 19468–19482.

Benjamini, Y., and Hochberg, Y. (1995). Controlling the false discovery rate: a practical and powerful approach to multiple testing. J. Roy. Stat. Soc. B *57*, 289–300.

Chan, F., Oatley, M.J., Kaucher, A.V., Yang, Q.-E., Bieberich, C.J., Shashikant, C.S., and Oatley, J.M. (2014). Functional and molecular features of the Id4+ germline stem cell population in mouse testes. Genes Dev. *28*, 1351–1362.

Claudel, T., Sturm, E., Duez, H., Torra, I.P., Sirvent, A., Kosykh, V., Fruchart, J.C., Dallongeville, J., Hum, D.W., Kuipers, F., et al. (2002). Bile acid-activated nuclear receptor FXR suppresses apolipoprotein A-I transcription via a negative FXR response element. J. Clin. Invest. *109*, 961–971.

Delbès, G., Levacher, C., Pairault, C., Racine, C., Duquenne, C., Krust, A., and Habert, R. (2004). Estrogen receptor beta-mediated inhibition of male germ cell line development in mice by endogenous estrogens during perinatal life. Endocrinology *145*, 3395–3403.

de Rooij, D.G., and Russell, L.D. (2000). All you wanted to know about spermatogonia but were afraid to ask. J. Androl. *21*, 776–798.

Gely-Pernot, A., Raverdeau, M., Teletin, M., Vernet, N., Féret, B., Klopfenstein, M., Dennefeld, C., Davidson, I., Benoit, G., Mark, M., et al. (2015). Retinoic acid receptors control spermatogonia cell-fate and induce expression of the SALL4A transcription factor. PLoS Genet. *11*, e1005501.

Griswold, M.D., and Oatley, J.M. (2013). Concise review: defining characteristics of mammalian spermatogenic stem cells. Stem Cells *31*, 8–11.

Hammoud, S.S., Nix, D.A., Zhang, H., Purwar, J., Carrell, D.T., and Cairns, B.R. (2009). Distinctive chromatin in human sperm packages genes for embryo development. Nature *460*, 473–478.

Hara, K., Nakagawa, T., Enomoto, H., Suzuki, M., Yamamoto, M., Simons, B.D., and Yoshida, S. (2014). Mouse spermatogenic stem cells continually interconvert between equipotent singly isolated and syncytial states. Cell Stem Cell *14*, 658–672.

Hosseinpour, B., Bakhtiarizadeh, M.R., Khosravi, P., and Ebrahimie, E. (2013). Predicting distinct organization of transcription factor binding sites on the promoter regions: a new genome-based approach to expand human embryonic stem cell regulatory network. Gene *531*, 212–219.

Huckins, C., and Oakberg, E.F. (1978). Morphological and quantitative analysis of spermatogonia in mouse testes using whole mounted seminiferous tubules, I. The normal testes. Anat. Rec. *192*, 519–528.

Id Boufker, H., Lagneaux, L., Fayyad-Kazan, H., Badran, B., Najar, M., Wiedig, M., Ghanem, G., Laurent, G., Body, J.J., and Journé, F. (2011). Role of farnesoid X receptor (FXR) in the process of differentiation of bone marrow stromal cells into osteoblasts. Bone *49*, 1219–1231.

Iwamori, N., Iwamori, T., and Matzuk, M.M. (2013). H3K27 demethylase, JMJD3, regulates fragmentation of spermatogonial cysts. PLoS One *8*, e72689.

Kaczmarek, K., Studencka, M., Meinhardt, A., Wieczerzak, K., Thoms, S., Engel, W., and Grzmil, P. (2011). Overexpression of peroxisomal testis-specific 1 protein induces germ cell apoptosis and leads to infertility in male mice. Mol. Biol. Cell *22*, 1766–1779.

Kim, D., Pertea, G., Trapnell, C., Pimentel, H., Kelley, R., and Salzberg, S.L. (2013). TopHat2: accurate alignment of transcriptomes in the presence of insertions, deletions and gene fusions. Genome Biol. *14*, R36.

Kratz, C.P., Han, S.S., Rosenberg, P.S., Berndt, S.I., Burdett, L., Yeager, M., Korde, L.A., Mai, P.L., Pfeiffer, R., and Greene, M.H. (2011). Variants in or near KITLG, BAK1, DMRT1, and TERT-CLPTM1L predispose to familial testicular germ cell tumour. J. Med. Genet. *48*, 473–476.

Langmead, B., and Salzberg, S.L. (2012). Fast gapped-read alignment with Bowtie 2. Nat. Methods *9*, 357–359.

Love, M.I., Huber, W., and Anders, S. (2014). Moderated estimation of fold change and dispersion for RNA-seq data with DESeq2. Genome Biol. *15*, 550.

Lui, W.Y., Mruk, D., Lee, W.M., and Cheng, C.Y. (2003). Sertoli cell tight junction dynamics: their regulation during spermatogenesis. Biol. Reprod. *68*, 1087–1097.

Maqdasy, S., El Hajjaji, F.Z., Baptissart, M., Viennois, E., Oumeddour, A., Brugnon, F., Trousson, A., Tauveron, I., Volle, D., Lobaccaro, J.M.A., et al. (2015). Identification of the functions of Liver X Receptor β in Sertoli cells using a targeted expression-rescue model. Endocrinology *156*, 4545–4557.

Milona, A., Owen, B.M., van Mil, S., Dormann, D., Mataki, C., Boudjelal, M., Cairns, W., Schoonjans, K., Milligan, S., Parker, M., et al. (2010). The normal mechanisms of pregnancy-induced liver growth are not maintained in mice lacking the bile acid sensor Fxr. Am. J. Physiol. Gastrointest. Liver Physiol. *298*, G151–G158.

Mu, W., Starmer, J., Fedoriw, A.M., Yee, D., and Magnuson, T. (2014). Repression of the soma-specific transcriptome by Polycomb-repressive complex 2 promotes male germ cell development. Genes Dev. *28*, 2056–2069.

Nakagawa, T., Sharma, M., Nabeshima, Y., Braun, R.E., and Yoshida, S. (2010). Functional hierarchy and reversibility within the murine spermatogenic stem cell compartment. Science *328*, 62–67.

Oatley, J.M., and Brinster, R.L. (2012). The germline stem cell niche unit in mammalian testes. Physiol. Rev. *92*, 577–595.

Omezzine, A., Chater, S., Mauduit, C., Florin, A., Tabone, E., Chuzel, F., Bars, R., and Benahmed, M. (2003). Long-term apoptotic cell death process with increased expression and activation of caspase-3 and -6 in adult rat germ cells exposed in utero to flutamide. Endocrinology *144*, 648–661.

Park, G.T., Seo, Y.M., Lee, S.Y., and Lee, K.A. (2012). Lin28 regulates the expression of neuropeptide Y receptors and oocyte-specific homeobox genes in mouse embryonic stem cells. Clin. Exp. Reprod. Med. *39*, 87–93.

Rizzo, G., Disante, M., Mencarelli, A., Renga, B., Gioiello, A., Pellicciari, R., and Fiorucci, S. (2006). The farnesoid X receptor promotes adipocyte differentiation and regulates adipose cell function in vivo. Mol. Pharmacol. *70*, 1164–1173.

Rust, C., Wild, N., Bernt, C., Vennegeerts, T., Wimmer, R., and Beuers, U. (2009). Bile acid-induced apoptosis in hepatocytes is caspase-6-dependent. J. Biol. Chem. *284*, 2908–2916.

Sanz, E., Evanoff, R., Quintana, A., Evans, E., Miller, J.A., Ko, C., Amieux, P.S., Griswold, M.D., and McKnight, G.S. (2013). RiboTag analysis of actively translated mRNAs in Sertoli and Leydig cells in vivo. PLoS One *8*, e66179.

Vega, A., Martinot, E., Baptissart, M., De Haze, A., Vaz, F., Kulik, W., Damon-Soubeyrand, C., Baron, S., Caira, F., and Volle, D.H. (2015). Bile acid alters male mouse fertility in metabolic syndrome context. PLoS One *10*, e0139946.

Volle, D.H., Duggavathi, R., Magnier, B.C., Houten, S.M., Cummins, C.L., Lobaccaro, J.M.A., Verhoeven, G., Schoonjans, K., and Auwerx, J. (2007a). The small heterodimer partner is a gonadal gatekeeper of sexual maturation in male mice. Genes Dev. *21*, 303–315.

Volle, D.H., Mouzat, K., Duggavathi, R., Siddeek, B., Déchelotte, P., Sion, B., Veyssière, G., Benahmed, M., and Lobaccaro, J.M.A. (2007b). Multiple roles of the nuclear receptors for oxysterols liver X receptor to maintain male fertility. Mol. Endocrinol. *21*, 1014–1027.

Volle, D.H., Decourteix, M., Garo, E., McNeilly, J., Fenichel, P., Auwerx, J., McNeilly, A.S., Schoonjans, K., and Benahmed, M. (2009). The orphan nuclear receptor small heterodimer partner

mediates male infertility induced by diethylstilbestrol in mice. J. Clin. Invest. *119*, 3752–3764.

West, J.A., Viswanathan, S.R., Yabuuchi, A., Cunniff, K., Takeuchi, A., Park, I.-H., Sero, J.E., Zhu, H., Perez-Atayde, A., Frazier, A.L., et al. (2009). A role for Lin28 in primordial germ-cell development and germ-cell malignancy. Nature *460*, 909–913.

Wilson, J.D., Leihy, M.W., Shaw, G., and Renfree, M.B. (2002). Androgen physiology: unsolved problems at the millennium. Mol. Cell. Endocrinol. *198*, 1–5.

Zheng, K., Wu, X., Kaestner, K.H., and Wang, P.J. (2009). The pluripotency factor LIN28 marks undifferentiated spermatogonia in mouse. BMC Dev. Biol. *9*, 38.

Stem Cell Reports, Volume *9*

Supplemental Information

The Bile Acid Nuclear Receptor FXRα Is a Critical Regulator of Mouse Germ Cell Fate

Emmanuelle Martinot, Lauriane Sèdes, Marine Baptissart, Hélène Holota, Betty Rouaisnel, Christelle Damon-Soubeyrand, Angélique De Haze, Jean-Paul Saru, Christelle Thibault-Carpentier, Céline Keime, Jean-Marc A. Lobaccaro, Silvère Baron, Gérard Benoit, Françoise Caira, Claude Beaudoin, and David H. Volle

A

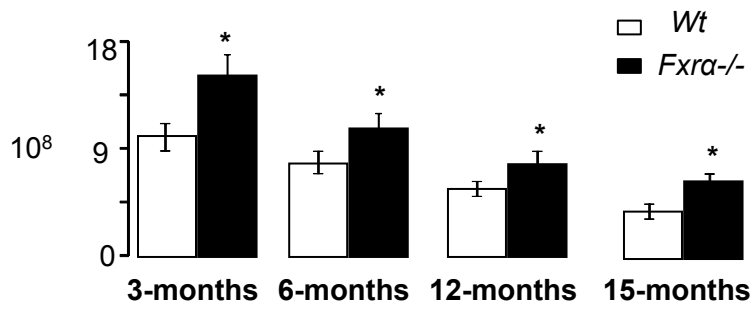

B

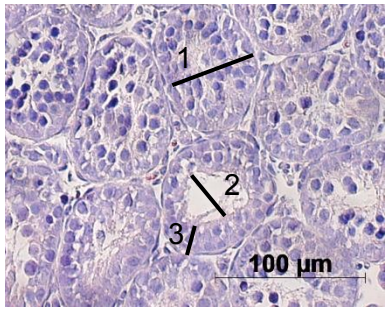

1: illustrate the diameter of the seminiferous tubule

2: illustrate the diameter of the lumen

3: illustrate the height of the epithelium

C

HE from 1 to 12 months

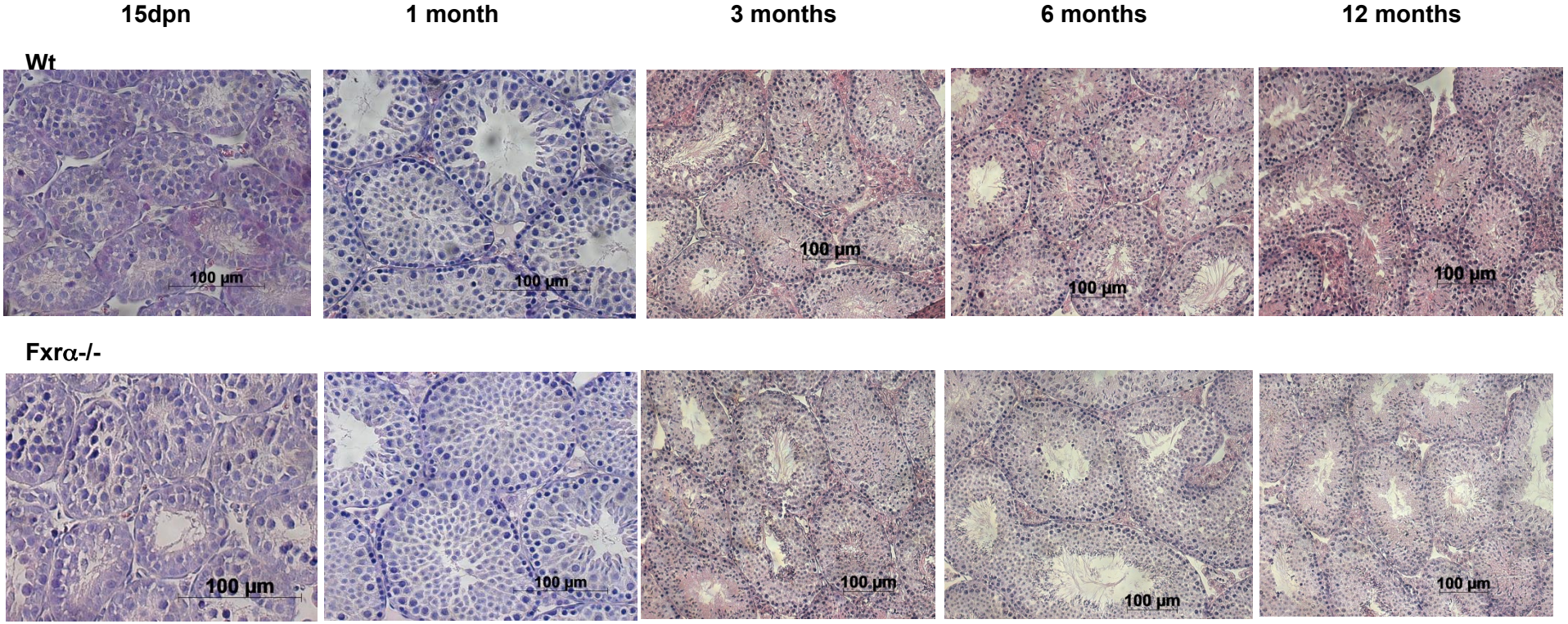

Suppl. 1

Figure S 1. Illustrates the sperm production and testicular histology, Related to Figure 1

A/ Relative number of sperm count in the epididymis head normalized to body weight in wild-type and *Fxrα*-/- at 3, 6, 12 or 15-month-old.

B/ A Representative image of a 10dpn testis; it is illustrate here the way how were quantified the diameter of the seminiferous tubule and the height of the epithelium.

C/ Representative images of a testis stained with eosine hematoxyline from wild-type and *Fxrα*-/- at 15dpn, 1, 3, 6, 12 or 15-month-old.

In all panel for each group, n =10 males from 3 to 4 independent litters; * denotes significance; $p<0.05$.

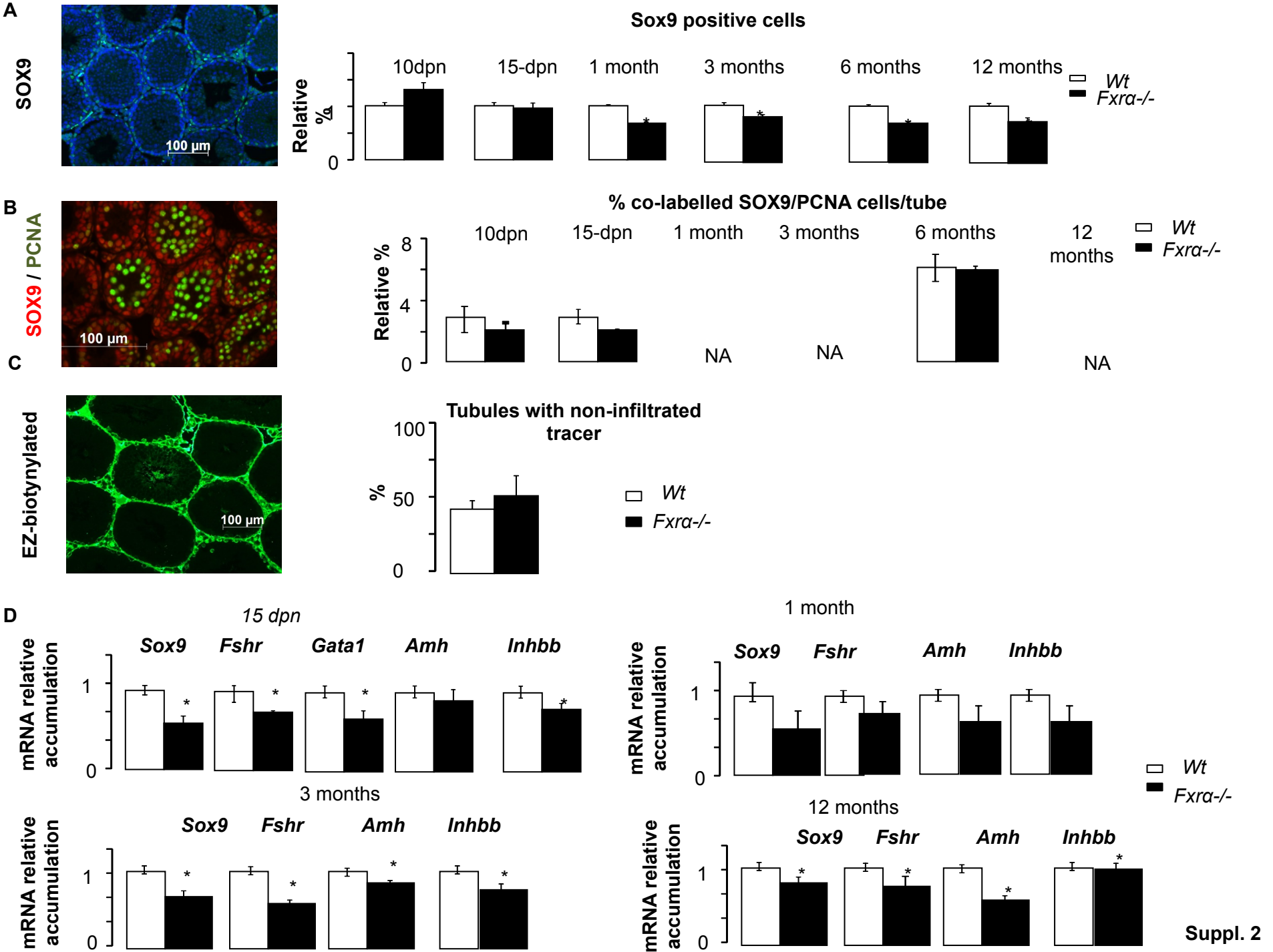
A
SOX9
100 µm
Sox9 positive cells
Relative %
0
10dpn
15-dpn
1 month
3 months
6 months
12 months
Wt
Fxrα-/-
B
SOX9 / PCNA
100 µm
% co-labelled SOX9/PCNA cells/tube
Relative %
8
4
0
10dpn
15-dpn
1 month
3 months
6 months
12 months
NA
NA
NA
Wt
Fxrα-/-
C
EZ-biotynylated
100 µm
Tubules with non-infiltrated tracer
%
100
50
0
Wt
Fxrα-/-
D
15 dpn
mRNA relative accumulation
Sox9
Fshr
Gata1
Amh
Inhbb
1
0
1 month
3 months
12 months
Wt
Fxrα-/-
Suppl. 2

Figure S 2. Impact of Fxrα deficiency on Sertoli cell homeostasis, Related to figure 2.

A/ Representative micrograph of the SOX9 staining in testis of Fxrα-/- male at 15 dpn. Quantification of the number of SOX9 positive cells is indicated as the number of positive cells per 100 seminiferous tubule in wild-type and Fxrα$^{-/-}$ mice at 10dpn, 15dpn, 1 months, 6 months and 12 months. **B/** Representative micrograph of the testis of 15-day-old *Fxrα-/-* male. Stained for PCNA and, SOX9. The original magnification was x200. Quantification of the percentage of cells co-labeled for PCNA and SOX9 per seminiferous tubule in wild-type and Fxrα$^{-/-}$ mice at 10dpn, 15dpn, 1 months, 6 months and 6 months. **C/** Representative micrograph of the efficiency of the BTB in testis of Fxrα$^{-/-}$ mice at 15 dpn visualized by staining of a biotynylated tracer. Quantification of the percentage of seminiferous tubules with tracer infiltration. **D/** Testicular mRNA accumulation of *Sox9*, *Fshr, Inhbb* and *Amh* normalized to β–actin mRNA levels in the whole testes of wild-type and Fxrα-/- mice at 15 days old, 1 month, 3 months and 12 months.

In all panels for each group, n =6 males from 4 independent litters; * denotes significance; $p<0.05$.

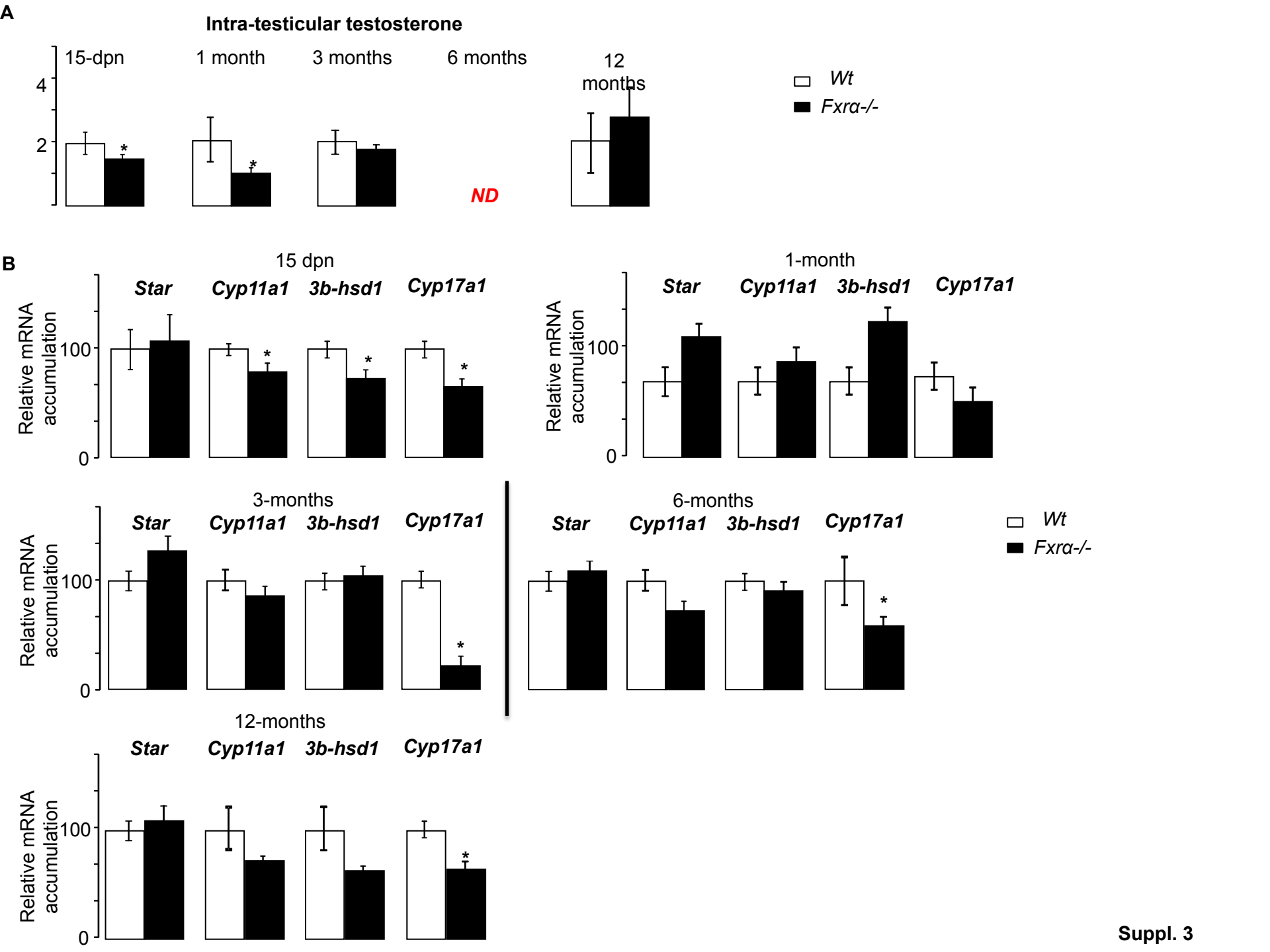
A
Intra-testicular testosterone
15-dpn
1 month
3 months
6 months
12 months
ND
Wt
Fxrα-/-
B
15 dpn
1-month
3-months
6-months
12-months
Star
Cyp11a1
3b-hsd1
Cyp17a1
Relative mRNA accumulation
100
0

Suppl. 3

Figure S 3. Impact of Fxrα deficiency on Leydig cell homeostasis, Related to figure 2.

A/ Intra-testicular testosterone concentrations in wild-type and Fxrα-/- mice at 15 dpn, 1 month, 3 months, 6 months and 12 months. **B/** Testicular mRNA accumulation of *Star*, *Cyp11a*1,*3β-Hsd1* and *Cyp17a1* normalized to *β–actin* mRNA levels in the whole testes of wild-type and Fxrα$^{-/-}$ mice at 15 dpn, 1 month, 3 months, 6 months and 12 months.

In all panels for each group, n =6 to 10 males from 4 to 5 independent litters; * denotes significance; $p<0.05$.

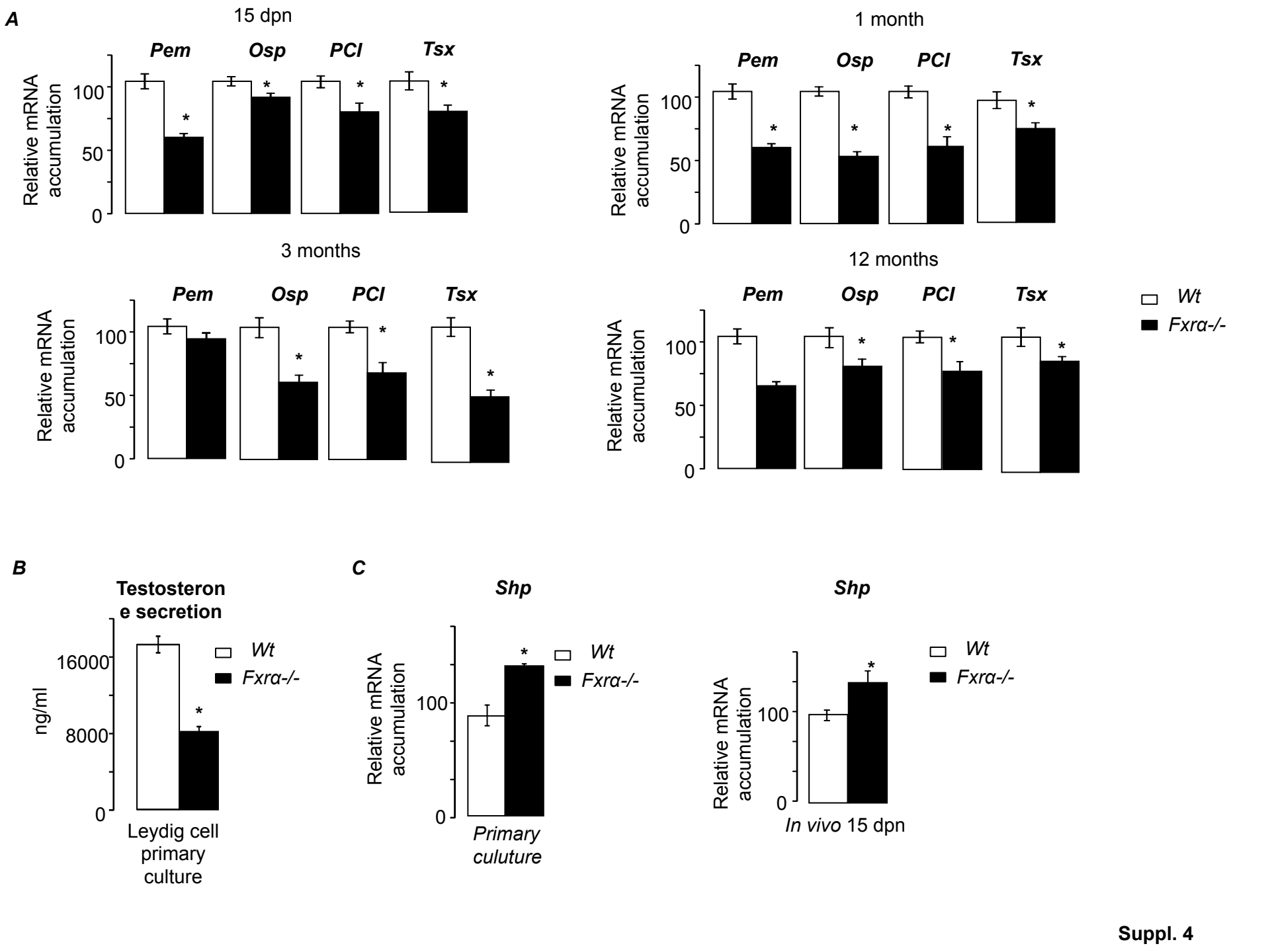
A
15 dpn
Pem
Osp
PCl
Tsx
Relative mRNA accumulation
100
50
0
*
1 month
3 months
12 months
Wt
Fxrα-/-
B
Testosteron e secretion
ng/ml
16000
8000
0
Leydig cell primary culture
C
Shp
Relative mRNA accumulation
Primary culuture
In vivo 15 dpn

Figure S 4. Impact of Fxrα deficiency on expression of androgeno-dependent genes, Related to figure 2.

A/ Testicular mRNA accumulation of *Pem*, *Osp*, *Pci* and *Tsx*normalized to *β–actin* mRNA levels in the whole testes of wild-type and Fxrα$^{-/-}$ mice at 15 dpn, 1 month, 3 months and 12 months. **B/** Testosterone secretion in Leydig cells (primary culture) from adult *wild-type* and *Fxrα*$^{-/-}$ mice. **C**/ mRNA accumulation of *Shp* normalized to *β–actin* mRNA levels evaluated in Leydig cells (primary culture) from 3 month-old *wild-type* and *Fxrα*$^{-/-}$ mice or in in the whole testes of wild-type and Fxrα$^{-/-}$ mice at 3 months.

In panels B and C, results were obtained from one experiment of primary culture from 20 Wt or 20 Fxrα-/- males.

In panel A & C, for in vivo experiments each group, n =6 males from 4 independent litters; * denotes significance; $p<0.05$.

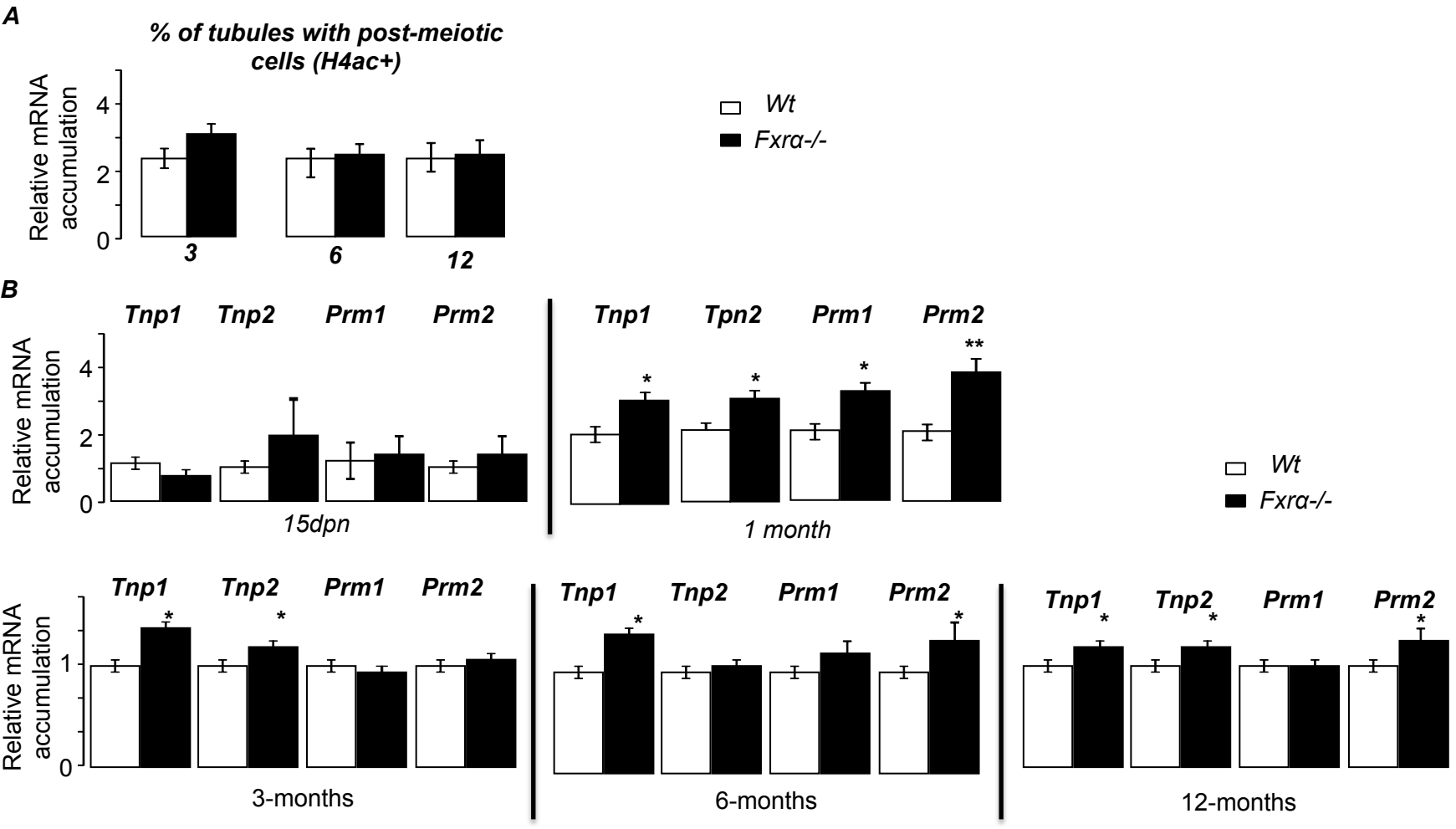
A
% of tubules with post-meiotic cells (H4ac+)
Relative mRNA accumulation
0
2
4
3
6
12
Wt
Fxrα-/-
B
Tnp1
Tnp2
Prm1
Prm2
Relative mRNA accumulation
15dpn
Tnp1
Tpn2
Prm1
Prm2
1 month
Wt
Fxrα-/-
Tnp1
Tnp2
Prm1
Prm2
Relative mRNA accumulation
0
1
3-months
Tnp1
Tnp2
Prm1
Prm2
6-months
Tnp1
Tnp2
Prm1
Prm2
12-months

Figure S 5. Fxrα deficiency improves germ cell differentiation, Related to figure 2.

A/ Quantification of the percentage of seminiferous tubules showing elongated H4ac positive germ cells in *wild-type* and *Fxrα*$^{-/-}$ mice from 3, 6 and 12 months of age.

B/ Testicular mRNA accumulation of *Tpn1, Tpn2, Prm1* and *Prm2* normalized to *β–actin* mRNA levels *wild-type* and *Fxrα*$^{-/-}$ mice at 15dpn, 1 month, 3 months and 12 months. .

In all panel for each group, n =5 to 10 males from 3 to 4 independent litters; * denotes significance; $p<0.05$.

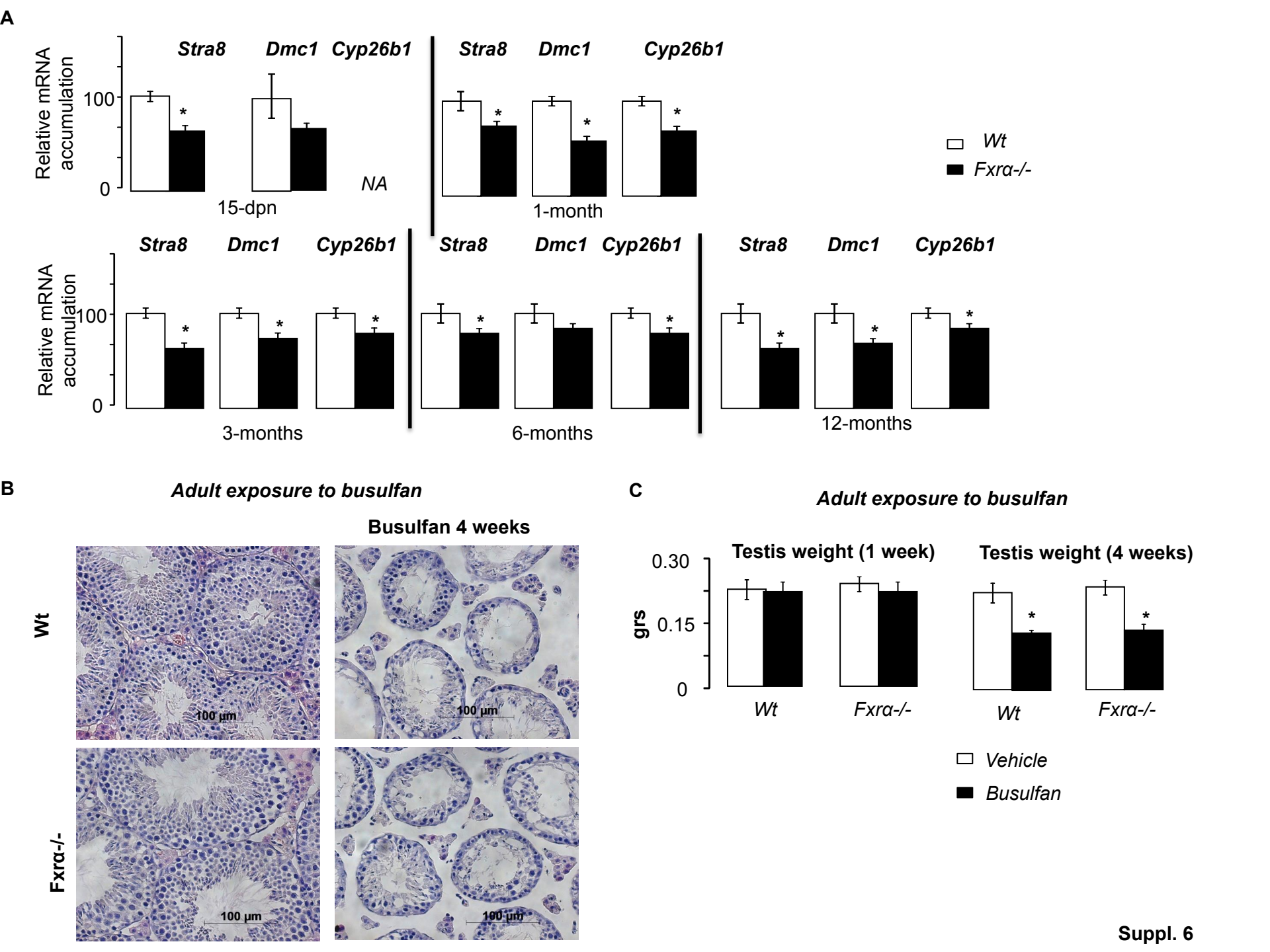
A
Relative mRNA accumulation
100
0
Stra8
Dmc1
Cyp26b1
*
NA
15-dpn
1-month
3-months
6-months
12-months
Wt
Fxrα-/-
B
Adult exposure to busulfan
Busulfan 4 weeks
Wt
Fxrα-/-
100 µm
C
Adult exposure to busulfan
Testis weight (1 week)
Testis weight (4 weeks)
grs
0.30
0.15
0
Vehicle
Busulfan

Suppl. 6

Figure S 6. Fxrα deficiency alters the expression of meiotic genes, Related to figure 3.

A/ Testicular mRNA accumulation of *Stra8*, *Dmc1 and Cyp26b1* normalized to *β–actin* mRNA levels in *wild-type* and *Fxrα*$^{-/-}$ mice at 15dpn, 1 month, 3 months, 6 months and 12 months. n=5-10 per group from 4 to 5 independent litters; * denotes significance; $p<0.05$. **B/** Representative micrographs of the testis H&E stained from 3 months old *wild-type* and *Fxrα-/-* mice treated with busulfan. **C/** Testis weights in *wild-type* and *Fxrα*-/- mice from 1 week and 4 weeks after busulfan exposure. In all panel n=5 to 6- per group from 3 different litters; * denotes significance; $p<0.05$.

A

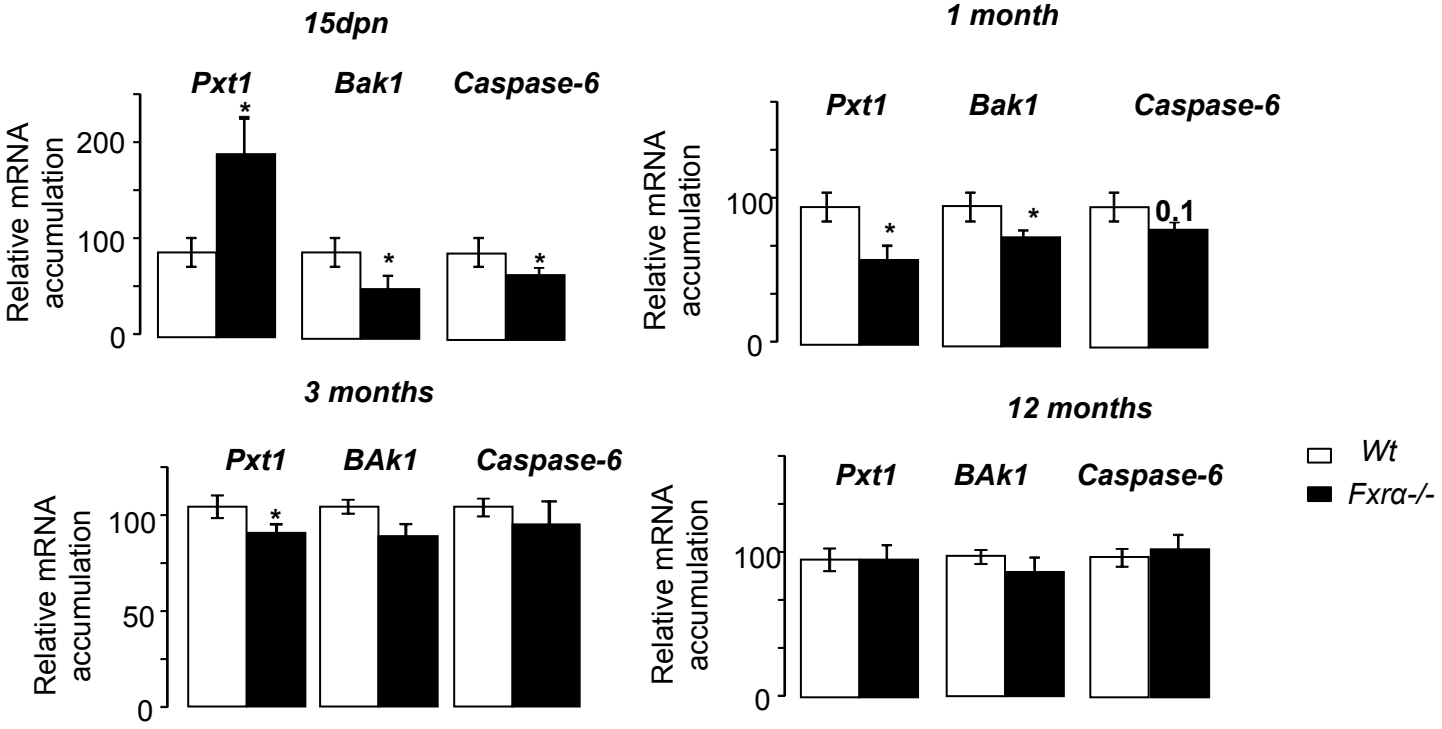
15dpn
Pxt1
Bak1
Caspase-6
Relative mRNA accumulation
200
100
0
1 month
100
0
0.1
3 months
BAk1
50
12 months
Wt
Fxrα-/-

B

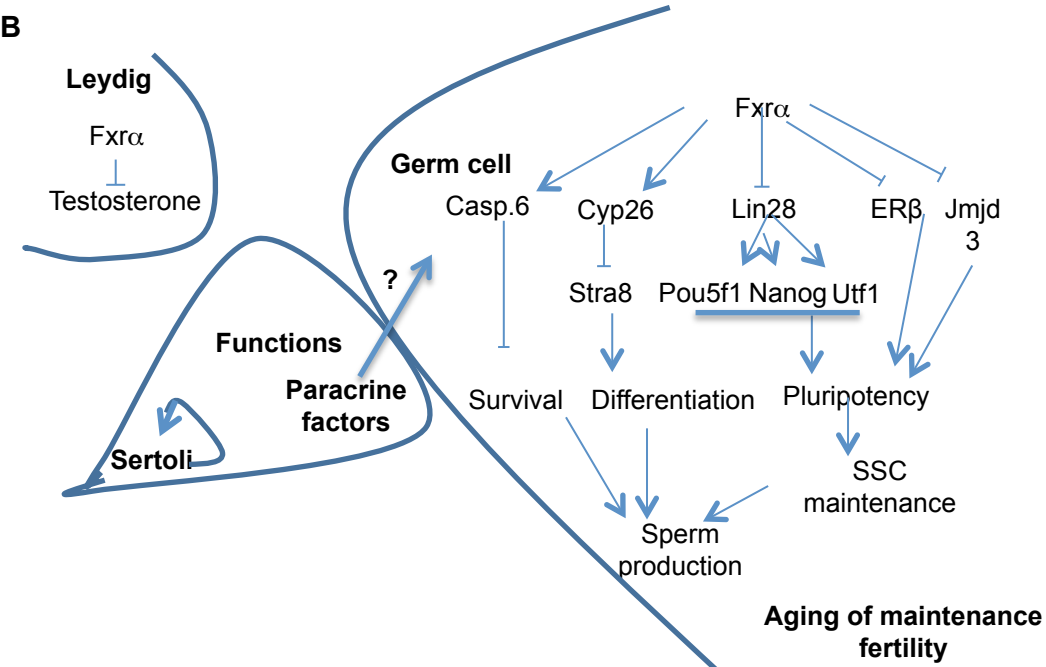
Leydig
Fxrα
Testosterone
Germ cell
Casp.6
Cyp26
Fxrα
Lin28
ERβ
Jmjd 3
Stra8
Pou5f1 Nanog Utf1
?
Functions
Paracrine factors
Sertoli
Survival
Differentiation
Pluripotency
SSC maintenance
Sperm production
Aging of maintenance fertility

Figure S 7. Fxrα deficiency alters the expression of genes involved in apoptosis, Related to figure 5

A/ Testicular mRNA accumulation of *Pxt1*, *Bak1 and Caspase-6* normalized to *β–actin* mRNA levels in the whole testes of wild-type and Fxrα$^{-/-}$ mice at 15 dpn, 1 month, 3 months, 6 months and 12 months. For each group, n =5 to 10 males from 3 to 4 independent litters; * denotes significance; $p<0.05$.

B/ Schematic model representing the putative roles of FXRα on testicular physiology**.**